

Engineering Arbitrary Hamiltonians in Phase Space

Lingzhen Guo¹ and Vittorio Peano¹

¹Max Planck Institute for the Science of Light, Staudtstrasse 2, 91058 Erlangen, Germany

(Dated: February 9, 2023)

We introduce a general method to engineer arbitrary Hamiltonians in the Floquet phase space of a periodically driven oscillator, based on the non-commutative Fourier transformation (NcFT) technique. We establish the relationship between an arbitrary target Floquet Hamiltonian in phase space and the periodic driving potential in real space. We obtain analytical expressions for the driving potentials in real space that can generate novel Hamiltonians in phase space, e.g., rotational lattices and sharp-boundary well. Our protocol can be realised in a range of experimental platforms for nonclassical states generation and bosonic quantum computation.

I. INTRODUCTION

Generation of nonclassical bosonic states [1–3], e.g., squeezed lights, Fock states and Schrödinger’s cat states, is important not only for fundamental studies of quantum mechanics but also for applications in quantum technologies [2, 4–6]. For example, bosonic states with discrete translational or rotational symmetries in phase space [7–14] have been proposed to encode quantum information [15–20], paving the way for hardware efficient quantum error correction [21–24]. Bosonic code states can be prepared and stabilized against dissipation via a sequence of universal gates, e.g. interleaved *selective number-dependent arbitrary phase* (SNAP) gates and displacement gates [25–27]. A fundamental limitation of this approach is that the state can leak out of the code and error subspaces [16, 20]. Hamiltonian engineering can solve this problem, allowing to design systems in which photon decay naturally leads into these subspaces [16, 28–30]. A further advantage of this approach is that the dephasing error for the ensuing logical qubit can be exponentially suppressed, allowing for fault tolerant syndrome detection [28].

Another area of interest for Hamiltonian engineering is topology. Due to the non-commutative nature of phase space, a quantum particle moving on a closed phase-space loop acquires a geometric phase analogous to the Ahronov-Bohm phase for a particles in a magnetic field. As a consequence, a gapped lattice Hamiltonian in phase space can support non-trivial Chern numbers [16, 31–39]. This is an appealing feature because in a system with a physical boundary, it would lead to topologically robust edge transport. While it has been shown how to generate arbitrary lattice potentials in phase-space [40], so far it was unclear how to combine such a potential with a sharp phase-space confinement.

It is well known that the stroboscopic dynamics of any periodically driven system can be described in terms of a time-independent Hamiltonian, known as *Floquet Hamiltonian* \hat{H}_F which is defined via

$$\exp\left(\frac{1}{i\lambda}\hat{H}_F T\right) \equiv \hat{U}(T, 0) = \mathcal{T} \exp\left[\frac{1}{i\lambda} \int_0^T \hat{H}(t) dt\right]. \quad (1)$$

Here, $\hat{U}(T, 0)$ is the time-evolution operator from $t = 0$ to $t = T$ where T is the time-period of the system’s time-dependent Hamiltonian $\hat{H}(t)$. In addition, λ is an effective dimensionless Planck constant, and \mathcal{T} is the time-ordering operator. For a single Bosonic mode or, equivalently, quantum mechanical particle, the Floquet Hamiltonian $H_F(\hat{x}, \hat{p})$ can be any arbitrary function in phase space. Except for very few models, it is impossible to obtain a closed form of the Floquet Hamiltonian $H_F(\hat{x}, \hat{p})$ from the time-dependent Hamiltonian $\hat{H}(t)$. Instead, one often evaluates the Floquet Hamiltonian relying on a high-frequency expansion [41–43], e.g. the Magnus expansion theory [44, 45], the van Vleck degenerate perturbation theory [46] and the Brillouin-Wigner perturbation theory [47]. In this work, we focus on the inverse problem, that is, to find the time-dependent Hamiltonian $\hat{H}(t)$ that synthesizes a target Floquet Hamiltonian $H_F^{(T)}(\hat{x}, \hat{p})$. This is the realm of Floquet engineering which is a very developed and active field [38, 48, 49]. Most of the work so far has focused on implementing specific Floquet Hamiltonians of interest. However, a systematic constructive method to solve the inverse Floquet problem for a single quantum particle is still missing. In this work, we provide such a method.

II. MODEL AND GOAL

As a starting point we consider a periodically driven oscillator with lab-frame Hamiltonian

$$\hat{\mathcal{H}}(t) = \frac{\omega_0}{2}(\hat{p}^2 + \hat{x}^2) + \beta V(\hat{x}, t). \quad (2)$$

Here, ω_0 is the oscillator natural frequency, β is the amplitude of the nonlinear driving potential $V(\hat{x}, t)$ which has time-period T_d and might contain also static terms. In order to introduce an effective dimensionless Planck constant λ , the position \hat{x} , the momentum \hat{p} and $\hat{H}_{\text{LF}}(t)$ have been rescaled such that $[\hat{x}, \hat{p}] = i\lambda$ and at the same time the Schrödinger equation reads $i\lambda\dot{\psi} = \hat{\mathcal{H}}(t)\psi$. The Floquet Hamiltonian we want to design will be defined in a frame rotating with the oscillator natural period $T = 2\pi/\omega_0$ via the transformation $\hat{O}(t) = \exp(i\hat{a}^\dagger \hat{a} \omega_0 t)$, where \hat{a} is the oscillator annihilation operator, $\hat{a} = (\hat{x} + i\hat{p})/\sqrt{2\lambda}$. We assume to be in the regime

of weak non-linearity, $\beta \ll \omega_0$, and that the natural period T is an integer multiple of the driving period T_d , $T = qT_d$. Then, the Hamiltonian in the rotating frame $\hat{H}(t) = \hat{O}(t)\hat{H}(t)\hat{O}^\dagger(t) - i\lambda O(t)\dot{O}^\dagger(t)$ reads

$$\hat{H}(t) = \beta V[\hat{x} \cos(\omega_0 t) + \hat{p} \sin(\omega_0 t), t]. \quad (3)$$

This Hamiltonian has time-period T allowing to use Eq. (1) to define the Floquet Hamiltonian. We note that a small detuning from the multiphoton resonance can be incorporated in the driving potential $V(x, t)$. In addition, the system in this frame evolves on the slow time-scale β^{-1} . Thus, we are in the realm of application of the Floquet high-frequency expansions, here, with the small parameter β/ω_0 . This allows to approximate the Floquet Hamiltonian with the leading-order of the Floquet-Magnus expansion corresponding to the rotating wave approximation (RWA),

$$\lim_{\omega_0 \rightarrow \infty} H_F(\hat{x}, \hat{p}) = \frac{1}{T} \int_0^T dt \hat{H}(t). \quad (4)$$

Our goal is to engineer an arbitrary target Floquet Hamiltonian $H_F^{(T)}(\hat{x}, \hat{p})$ in phase space by properly designing the driving potential $V(x, t)$ in real space, see Fig. 1. Up to leading order (or within the RWA) we, thus, require that the right-hand side of Eq. (4) coincides with the target Hamiltonian $H_F^{(T)}(\hat{x}, \hat{p})$. The ensuing solution becomes exact in the high-frequency limit $\beta/\omega_0 \rightarrow 0$.

III. NcFT TECHNIQUE

As a preliminary step towards deriving a suitable driving potential $V(x, t)$, we introduce a useful decomposition of the target Hamiltonian $H_F^{(T)}(\hat{x}, \hat{p})$ in the form of a *noncommutative Fourier transformation* (NcFT). This can be viewed as a variant of quantum distribution theory [50]. We wish to decompose the target Hamiltonian $H_F^{(T)}(\hat{x}, \hat{p})$ as a sum of plane-wave operators

$$H_F^{(T)}(\hat{x}, \hat{p}) = \frac{\beta}{2\pi} \iint dk_x dk_p f_T(k_x, k_p) e^{i(k_x \hat{x} + k_p \hat{p})}. \quad (5)$$

It can be shown that the Fourier coefficients $f_T(k_x, k_p)$ are given by the inverse transformation [see the Appendix A]

$$f_T(k_x, k_p) = \frac{e^{\frac{\lambda}{4}(k_x^2 + k_p^2)}}{2\pi\beta} \iint dx dp H_Q^{(T)}(x, p) e^{-i(k_x x + k_p p)}, \quad (6)$$

where the phase-space function $H_Q^{(T)}(x, p)$ is the equivalent of the Husimi Q-function, here, for an Hamiltonian instead of the density operator. We remind that the Q-function of an operator evaluated at a phase space point (x, p) is simply its expectation value $H_Q^{(T)}(x, p) = \langle \alpha | \hat{H}_F^{(T)} | \alpha \rangle$ for the corresponding coherent state $\hat{a} | \alpha \rangle =$

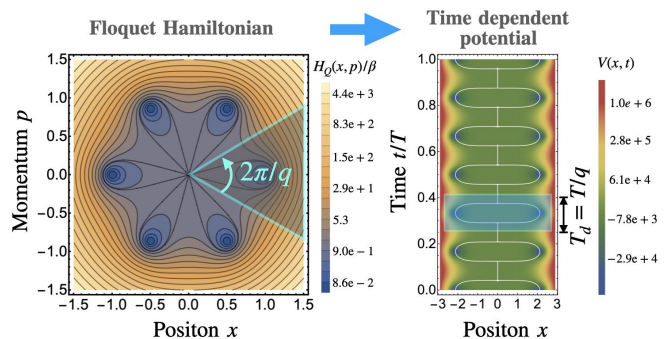


FIG. 1: **Rotational lattice Hamiltonian in phase space.** (Left) Q-function $H_Q^{(T)}(x, p)$ for the target Floquet Hamiltonian Eq. (9) and (Right) the engineered real-space potential $V(x, t)$ for parameters $q = 6$, $\lambda = 0.01$. The white curves in the right figure indicate the locations of minimum (stable) points of $V(x, t)$ at a fixed time moment.

$(x + ip) | \alpha \rangle / \sqrt{2\lambda}$. The latter mean value can be calculated by normal ordering the target Hamiltonian $\hat{H}_F^{(T)}(\hat{a}^\dagger, \hat{a})$. We point out three important features of the Hamiltonian Q-function: (i) For fixed λ , the mapping between Floquet Hamiltonians and Q-functions is one to one; (ii) The Hamiltonian Q-function has the same phase-space symmetries as the corresponding Floquet Hamiltonian, and (iii) $\lim_{\lambda \rightarrow 0} H_Q^{(T)}(x, p) = H_F^{(T)}(x, p)$. For more details see the Appendix B and Appendix H.

IV. DESIGNING DRIVING POTENTIAL

The driving potential $V(x, t)$ that generates the target Floquet Hamiltonian $H_F^{(T)}(\hat{x}, \hat{p})$ can be readily obtained from its Fourier coefficient $f_T(k_x, k_p)$. We can formally write the solution as a superposition of sinusoidal potentials

$$V(x, t) = \int_0^{+\infty} A(k, \omega_0 t) \cos[kx + \phi(k, \omega_0 t)] dk \quad (7)$$

with time-varying amplitudes $A(k, \tau)$ and phases $\phi(k, \tau)$ determined from the Fourier coefficients in polar coordinates ($k_x = k \cos \tau$, $k_p = k \sin \tau$)

$$A = k |f_T(k \cos \tau, k \sin \tau)|, \quad \phi = \text{Arg} f_T(k \cos \tau, k \sin \tau). \quad (8)$$

This solution can be readily verified by plugging it into Eqs. (3) and (4), and changing the integration variables back to cartesian coordinates to arrive at Eq. (5). For more details see the Appendix C. In the remainder of this paper, we demonstrate the flexibility of our method calculating the potential $V(x, t)$ for a range of interesting Floquet Hamiltonians. In passing, we will also highlight more general features of our solution and comment on certain subtleties associated with it.

V. EXAMPLES

A. Rotational lattice

We now apply our method to synthesize a particularly interesting Floquet Hamiltonian with q -fold rotational lattice symmetry in phase space

$$\hat{H}_F^{(T)} = \beta [(\hat{x} - i\hat{p})^q - 1] [(\hat{x} + i\hat{p})^q - 1]. \quad (9)$$

The discrete rotational symmetry can be described by $\hat{R}(\frac{2\pi}{q})\hat{H}_F^{(T)}\hat{R}(\frac{2\pi}{q}) = \hat{H}_F^{(T)}$, where $\hat{R}(\theta) = \exp(i\hat{a}^\dagger\hat{a}\theta)$ is a phase-space rotation by an angle θ [20, 36]. This Hamiltonian supports q global minima, cf. the Q -function in Fig. 1 (left) for $q = 6$. Here, we have rescaled the phase-space coordinates such that the global minima fulfill $|x + ip| = 1$. Each minimum corresponds to a different classical solution. Remarkably, quantum fluctuations do not introduce any tunneling between these solutions as the corresponding coherent states $|\alpha\rangle = |e^{im\frac{2\pi}{q}}/\sqrt{2\lambda}\rangle$ with $m = 0, 1, \dots, q-1$ are exact zero-energy eigenstates. In other words, the groundstate manifold is q -dimensional and is spanned by q q -legged cat states. The oscillator is steered into this manifold by photon decay (see the Appendix E). The case $q = 2$ has been proposed as a platform for fault tolerant syndrome detection [28].

Note that since the Hamiltonian Q -function is a polynomial, its Fourier transform Eq. (6) is divergent. To solve this problem, we renormalize the divergence introducing the bounded Hamiltonian $\hat{H}_{F\gamma}^{(T)} = U_\gamma\hat{H}_F^{(T)}U_\gamma^\dagger$ with $U_\gamma = \exp[-\gamma\hat{a}^\dagger\hat{a}]$. Obviously, $\lim_{\gamma\rightarrow 0}\hat{H}_{F\gamma}^{(T)} = \hat{H}_F^{(T)}$. We can calculate analytically $f_T(k_x, k_p)$ and $V(x, t)$ for $\hat{H}_{F\gamma}^{(T)}$ for any arbitrary positive integer q and $\gamma > 0$. In the limit $\gamma \rightarrow 0$, the Fourier transform can be viewed as a generalized function. This allows to perform the integral in Eq. (7) and arrive at a closed expression for the driving potential (for more details see the Appendix D)

$$V(x, t) = \sum_{m=1}^q B_{q,m}\lambda^{q-m}x^{2m} - C_q \cos(q\omega_0 t)x^q, \quad (10)$$

with $B_{q,m} = \frac{(2^m q!)^2 (-1)^{q+m}}{(2m)!(q-m)!}$ and $C_q = \frac{2\sqrt{\pi}q!}{\Gamma[(2q+3-(-1)^q)/4]}$. We note that for $q = 2$ we recover a well-known result: Eq. (10) corresponds to a parametrically driven Duffing oscillator [51–54]. We further note that the driving period is $T_d = T/q$ which directly follows from the q -fold rotational symmetry of the Floquet Hamiltonian.

B. Sharp-boundary well

Next, we demonstrate that our method allows to engineer wells with a sharp boundary in phase space. For concreteness we choose an elliptical shape, i.e. $H_Q^{(T)}(x, p) = -\beta$ inside the white dashed line in Fig. 2(a) and $H_Q^{(T)} = 0$

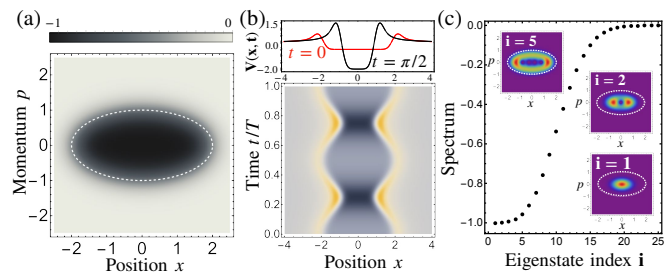


FIG. 2: **Elliptical well in phase space.** (a) Hamiltonian Q -function $H_Q^{(T)}(x, p)/\beta$ with long axis $a = 2$, short axis $b = 1$, $\lambda = 0.1$ and convolution factor $\sigma = \sqrt{\lambda}$. (b) Designed driving potential $V(x, t)$ in one Floquet period (lower) and at instants $t = 0, t = \pi/2$ (upper). (c) Energy spectrum and Husimi Q -functions of ground state ($i = 1$), first excited state ($i = 2$), fourth ($i = 5$) excited eigenstates. The dashed circles in (a) and (c) indicate the boundary of elliptical well.

otherwise. In the classical limit $\lambda \rightarrow 0$, our method allows to find a closed form solution for $V(x, t)$ (see Appendix F). However, our solution is divergent at two time-dependent positions. In addition, it does not directly apply to the quantum regime, $\lambda \neq 0$, because the dependence of $V(x, t)$ on λ is not analytical. This is due to the exponential factor in Eq. (6) leading to divergent NcFT coefficients $f_T(k_x, k_p)$ in the limit of large wavevectors, $k_x^2 + k_p^2 \rightarrow \infty$, for any $\lambda \neq 0$. We eliminate these unphysical features by smoothing out the target Floquet Hamiltonian applying a convolution with a gaussian kernel with standard deviation σ , cf. Fig. 2(a). For σ above a threshold, $\sigma > \sqrt{\lambda/2}$, the NcFT spectrum $f_T(k_x, k_p)$ becomes integrable and, thus, leads to a smooth solution for $V(x, t)$, cf. Fig. 2(b) and the closed expression in the Appendix F. This implies that we can implement a potential step that is arbitrarily sharp when compared to the typical dimensions of the phase-space well, but should remain smooth on the scale of the oscillator quantum fluctuations. We point out that a sharp boundary narrower than quantum fluctuations ($\sigma < \sqrt{\lambda/2}$) does exist (Hamiltonian matrix elements in Fock presentation are well defined, see Appendix B and Appendix F) but cannot be realised by our present method. The spectrum and first few eigenmodes are also shown in Fig. 2(c). The latter are squeezed non-gaussian states.

C. Moiré superlattice

In Ref [40], we have shown how to synthesize arbitrary lattices in phase space. We can use our method to combine a lattice potential with a sharp confinement realizing a finite size lattice. For concreteness we focus on a Moiré superlattice, cf. Fig. 3(a). This is the phase-space equivalent of the 2D potential for electrons in twisted graphene [55–58]. The Moiré superlattice is formed by overlaying two honeycomb lattices with a relative twist angle

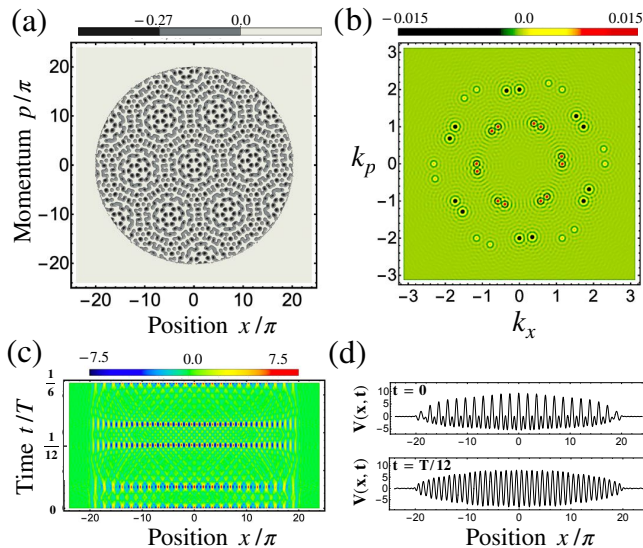


FIG. 3: **Moiré superlattice in phase space.** (a) Hamiltonian Q-function of Moiré superlattice with twisted angle $\theta = 10^\circ$ and confined in a region with radius $R = 20\pi$. (b) Density plot of NcFT coefficient $\beta f_T(k_x, k_p)$. (c) Designed driving potential $V(x, t)$ for $t \in [0, T/6)$. (d) $V(x, t)$ at fixed time instants $t = 0$ (upper) and $t = T/12$ (lower).

θ_0 in a finite region of radius R . Outside of this region $H_F^{(T)}(x, p) = 0$. The resulting Hamiltonian Q-function for the twist angle $\theta_0 = 10^\circ$ is shown in Fig. 3(a). As discussed above, overall the Floquet Hamiltonian should be smooth on the scale of the oscillator quantum fluctuations. As for the phase-space well example above, this can be implemented applying a convolution with a gaussian kernel to the initially discontinuous Floquet Hamiltonian. The ensuing transition between the Floquet lattice potential and the phase-space region with $H_F^{(T)}(x, p) = 0$ can be arbitrarily sharp compared to R or to the honeycomb lattice constant (in our dimensionless phase-space coordinates the lattice constant is π). A closed formula for the Floquet Hamiltonian is given in the Appendix G.

Applying our method, we calculate the NcFT spectrum $f_T(k_x, k_p)$ shown in Fig. 3(b). It is formed by three groups of twelve peaks. Each group of peaks is obtained from a single peak by applying one of the six-fold phase-space rotations and/or the rotation by the twist angle θ_0 , cf Fig. 3(a). The width of all the peaks is $\propto R^{-1}$. All these features as well as the exact locations of the peaks can be read out from a closed form solution for $f_T(k_x, k_p)$ given in the Appendix G. In Fig. 3(c), we plot the ensuing driving potential $V(x, t)$ for $0 \leq t < T_d$. [In this case, the driving period T_d is one sixth of the natural period, $T_d = T/6$, reflecting the 6-fold rotational-symmetry of our target Floquet Hamiltonian.] In Fig. 3(d), we also plot the instant driving potential at $t = 0$ and $t = T_d/2$ (or $t = T/12$). We note that the real-space driving potential is a sequence of discrete lattice potentials localized

in a finite region of real space that are switched on for a short time interval. We note further that in the limit $R \rightarrow \infty$, the peaks in (k_x, k_p) -space become δ -functions and the driving potential reduces to a discrete sequence of stroboscopic lattices with specific amplitudes, wavelengths and phases [38, 40, 59, 60]. Considering that the contact interaction of cold atoms turns into a long-distance Coulomb-like interaction in the rotating frame [38, 40, 60–66], many atoms in the phase space Moiré superlattice would mimic the behaviour of electrons in twisted bilayer graphene [55–58].

D. Artificial atomic spectrum

As a final application, we show that our method allows to implement a target spectrum $\{E_n\}$ as well as desired target eigenstates $\{|\psi_n\rangle\}$. As mentioned above, this could be useful for quantum simulations with interacting atoms. In this scenario, our method could be straightforwardly applied to the target Floquet Hamiltonian $\hat{H}_F^{(T)} = \sum_n E_n |\psi_n\rangle\langle\psi_n|$. For concreteness, we consider $|\psi_n\rangle = |n\rangle$ where $\{|n\rangle\}$ is the harmonic oscillator (Fock states) eigenbasis. In this example, the Hamiltonian Q-function and the NcFT spectrum can be easily expressed as a sum over the excitation number n ,

$$H_Q^{(T)}(x, p) = e^{-\frac{x^2+p^2}{2\lambda}} \sum_{n=0}^{\infty} \frac{E_n}{n!} \left(\frac{x^2+p^2}{2\lambda}\right)^n, \quad (11)$$

and

$$f_T(k_x, k_p) = \sum_{n=0}^{\infty} \lambda \frac{E_n}{\beta} e^{\lambda \frac{k^2}{4}} {}_1F_1(1+n; 1; -\lambda \frac{k^2}{2}), \quad (12)$$

respectively. Here, ${}_1F_1(a; b; z)$ is the Kummer confluent hypergeometric function. The driving potential $V(x)$ can be straightforwardly calculated by plugging Eq. (12) into Eqs. (7) and (8). Note that since the NcFT spectrum $f_T(k \cos \tau, k \sin \tau)$ is independent of the angular coordinate τ , the driving potential $V(x)$ is *static*. This, in turn, follows from our choice of eigenbasis leading to a target Floquet Hamiltonian invariant under arbitrary phase-space rotations, cf. Eq. (11). Note further that the asymptotic behavior ${}_1F_1(1+n; 1; -\frac{k^2}{2}) \sim (-\frac{\lambda k^2}{2n!})^n e^{-\frac{\lambda k^2}{2}}$ for $k \rightarrow \infty$ ensures that the integral in Eq. (7) is well defined. In Fig. 4 we display the potential $V(x)$ for two interesting choices of the spectrum $\{E_n\}$. In panel (a), we fix $\{E_n\}$ to be the spectrum of the hydrogen atom $E_n = -\beta\lambda/(n+1)^2$. In panel (b) we choose $E_1 = -\beta\lambda$ and $E_0 = E_1 - \beta\lambda(\lambda - \frac{3}{4})$ while all other levels are zero, $E_{n>1} = 0$. Thus, at $\lambda = 3/4$, the energies E_0 and E_1 of the second spectrum display an exact crossing.

VI. EXPERIMENTAL IMPLEMENTATIONS

In order to design arbitrary Hamiltonians in phase space, one needs the ability to engineer the driving real-

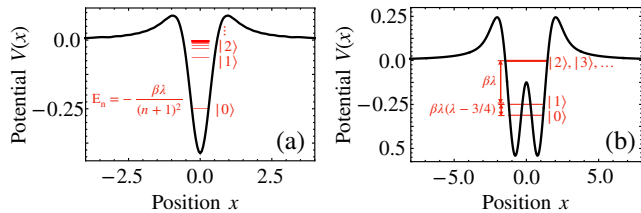


FIG. 4: **Artificial spectrum:** (a) designed hydrogen atomic levels with parameter $\lambda = \frac{1}{4}$; (b) levels $|0\rangle$ and $|1\rangle$ gapped from other degenerate levels with $\lambda = 1$. In both figures, the eigenstates $|n\rangle$ are the harmonic Fock states.

space potential $V(x, t)$ in experiments. As discussed above, cf. Eq. (7), the driving potential can be engineered by superposing a series of cosine lattice potentials with tunable amplitudes, wave vectors and phases. In cold atom experiments, this can be done with optical lattices that are formed by laser beams intersecting at an angle [40, 67, 68]. In experiments with superconducting circuits [69–71], a microwave cavity in series with a Josephson junction (JJ) biased by a dc voltage (V) is described by the Hamiltonian $\hat{\mathcal{H}}(t) = \hbar\omega_0\hat{a}^\dagger\hat{a} - E_J \cos[\omega_J t + \Delta(\hat{a}^\dagger + \hat{a})]$, where E_J is the JJ energy, $\omega_J = 2eV/\hbar$ is the Josephson frequency and $\Delta = \sqrt{2e^2/(\hbar\omega_0 C)}$ with C the cavity capacitance [72–83]. In principle, more complicated driving potential can be realized using more JJs and electric

elements.

VII. SUMMARY AND OUTLOOK

In this work, we have introduced a powerful tool for Floquet engineering: A general constructive method to derive the driving potential $V(x, t)$ generating any arbitrary target Floquet Hamiltonian $H_F^{(T)}(x, p)$ of a single Bosonic mode. Here, we provide an approximation for $V(x, t)$ up to leading order in the high-frequency Floquet-Magnus expansion. A natural extension of our work would be to include higher-order perturbative corrections, which can be viewed as the inverse problem of the Floquet-Magnus theory. Another exciting prospect is to extend our method to a many-body scenario. A building block for this extension is to upgrade the single-particle plane-wave operator $\exp[i(k_x\hat{x} + k_p\hat{p})]$ used in the NcFT Eq. (5) to a many-body equivalent, $\exp[\sum_j i(k_x^j\hat{x}_j + k_p^j\hat{p}_j)]$ where (\hat{x}_j, \hat{p}_j) are the phase-space coordinates of the j -th particle. In experiments with superconducting circuits, this could be implemented coupling a dc-voltage biased JJ to multiple superconducting cavities [72, 77, 78, 80, 81, 83].

Acknowledgements

We acknowledge helpful discussions with Florian Marquardt and Muxin Han.

Appendix A: Noncommutative Fourier transformation

In this section, we provide detailed calculation of the noncommutative Fourier transformation (NcFT) coefficient for a given target Floquet Hamiltonian operator $\hat{H}_F^{(T)} = H_F^{(T)}(\hat{x}, \hat{p})$. We start from writing the target Hamiltonian as a sum of plane-wave operators, cf. Eq. (5) in the main text,

$$H_F^{(T)}(\hat{x}, \hat{p}) = \frac{\beta}{2\pi} \int \int dk_x dk_p f_T(k_x, k_p) e^{i(k_x\hat{x} + k_p\hat{p})}. \quad (\text{A1})$$

In order to calculate the Fourier coefficient $f_T(k_x, k_p)$, we first express the target Hamiltonian with reordered ladder operators

$$H_F^{(T)}(\hat{a}^\dagger, \hat{a}) \equiv \sum_{n,m} \chi_{nm} (\hat{a}^\dagger)^n \hat{a}^m.$$

Note that the ordering here keeps all the terms from commutators. By defining the coherent state $|\alpha\rangle$ as the eigenstate of lowering operator $\hat{a}|\alpha\rangle = \alpha|\alpha\rangle$, we calculate the operator in the diagonal coherent representation

$$H_Q^{(T)}(\alpha, \alpha^*) \equiv \langle \alpha | \hat{H}_F^{(T)} | \alpha \rangle = \sum_{n,m} \chi_{nm} (\alpha^*)^n \alpha^m. \quad (\text{A2})$$

Function $H_Q^{(T)}(\alpha, \alpha^*)$ can also be written as $H_Q^{(T)}(x, p)$ by identifying $\alpha = (x + ip)/\sqrt{2\lambda}$ where

$$\begin{cases} x \equiv \langle \alpha | \hat{x} | \alpha \rangle = \sqrt{\frac{\lambda}{2}}(\alpha^* + \alpha) \\ p \equiv \langle \alpha | \hat{p} | \alpha \rangle = i\sqrt{\frac{\lambda}{2}}(\alpha^* - \alpha). \end{cases} \quad (\text{A3})$$

In order to calculate the NcFT coefficient $f_T(k_x, k_p)$ in Eq. (A1), we need to calculate the coherent diagonal element of the plane-wave operator $\langle \alpha | e^{i(k_x\hat{x} + k_p\hat{p})} | \alpha \rangle$. For this purpose, we introduce the displacement operator

$\hat{D}_\alpha \equiv e^{\alpha \hat{a}^\dagger - \alpha^* \hat{a}}$ with the following relationship [65]

$$D_\alpha D_\beta = e^{i\text{Im}(\alpha\beta^*)} D_{\alpha+\beta}, \quad D_\alpha |\beta\rangle = e^{i\text{Im}(\alpha\beta^*)} |\alpha + \beta\rangle. \quad (\text{A4})$$

We then write the plane-wave operator as $e^{i(k_x \hat{x} + k_p \hat{p})} = \hat{D}_{-\sqrt{\frac{\lambda}{2}}(k_p - ik_x)}$. Using the relationship (A4), we have the matrix element of plane-wave operator $e^{i(k_x \hat{x} + k_p \hat{p})}$ in coherent state representation

$$\begin{aligned} \langle \alpha | e^{i(k_x \hat{x} + k_p \hat{p})} | \beta \rangle &= \langle \alpha | \hat{D}_{-\sqrt{\frac{\lambda}{2}}(k_p - ik_x)} | \beta \rangle \\ &= \left\langle \alpha \left| \beta - \sqrt{\frac{\lambda}{2}}(k_p - ik_x) \right. \right\rangle e^{-i\sqrt{\frac{\lambda}{2}}\text{Im}[(k_p - ik_x)\beta^*]} \\ &= e^{-\frac{1}{2}|\alpha|^2 - \frac{1}{2}|\beta - \sqrt{\frac{\lambda}{2}}(k_p - ik_x)|^2 + \alpha^* \beta - \alpha^* \sqrt{\frac{\lambda}{2}}(k_p - ik_x) - i\sqrt{\frac{\lambda}{2}}\text{Im}[(k_p - ik_x)\beta^*]} \end{aligned} \quad (\text{A5})$$

In the last step, we have used and the identity $\langle \alpha | \beta \rangle = e^{-|\alpha|^2/2 - |\beta|^2/2 + \alpha^* \beta}$. Thus, we have the diagonal elements of plane-wave operator from Eq. (A5)

$$\langle \alpha | e^{i(k_x \hat{x} + k_p \hat{p})} | \alpha \rangle = \exp\left(-\frac{\lambda}{4}|k_p - ik_x|^2\right) e^{i(k_x x + k_p p)} = e^{-\frac{\lambda}{4}(k_x^2 + k_p^2)} e^{i(k_x x + k_p p)}. \quad (\text{A6})$$

Using Eqs. (A2) and (A6), we have the Fourier coefficient from Eq. (A1) as follows

$$f_T(k_x, k_p) = \frac{e^{\frac{\lambda}{4}(k_x^2 + k_p^2)}}{2\pi\beta} \int \int dx dp H_Q^{(T)}(x, p) e^{-i(k_x x + k_p p)}. \quad (\text{A7})$$

Eqs. (A1) and (A7) construct the noncommutative Fourier transformation (NcFT) technique introduced in this paper. From the hermicity of Hamiltonian operator, we have the following important relationship

$$f_T(k_x, k_p) = f_T^*(-k_x, -k_p). \quad (\text{A8})$$

Note out that here we present a general way to calculation the NcFT coefficient. In practice, for some specific target Hamiltonians, there may exist a simpler and more direct way to obtain the result as for the rotational lattice shown below.

Appendix B: One-to-one correspondence between Hamiltonian operator and Q-function

In the above derivation of the NcFT coefficient for a given target Hamiltonian operator, we perform Fourier transformation of the Hamiltonian Q-function that only takes the diagonal elements of Hamiltonian operator in the coherent state representation, cf. Eq. (A2). One may wonder if some information is lost by neglecting the off-diagonal elements. In this section, we will prove the Hamiltonian operator $H_F^{(T)}(\hat{x}, \hat{p})$, given by Eqs. (A1) and (A7), is fully determined by its Hamiltonian Q-function $H_Q^{(T)}(x, p) \equiv \langle \alpha | H_F^{(T)}(\hat{x}, \hat{p}) | \alpha \rangle$ together with commutator $[\hat{x}, \hat{p}] = i\lambda$.

We write the Hamiltonian in the Fock representation $\hat{H}_F^{(T)} = \sum_{n,m} \xi_{nm} |n\rangle \langle m|$ with $n, m = 0, 1, \dots$ and define the following operator

$$H_{nm}(\hat{x}, \hat{p}) \equiv \frac{1}{2\pi} \int \int dk_x dk_p f_{nm}(k_x, k_p) e^{i(k_x \hat{x} + k_p \hat{p})}. \quad (\text{B1})$$

where $f_{nm}(k_x, k_p)$ is the NcFT coefficient of the operator $|n\rangle \langle m|$ given by

$$f_{nm}(k_x, k_p) = \frac{e^{\frac{\lambda}{4}(k_x^2 + k_p^2)}}{2\pi} \int \int dx dp H_{nm}(x, p) e^{-i(k_x x + k_p p)} \quad (\text{B2})$$

with the Q-function of operator $|n\rangle \langle m|$ given by

$$H_{nm}(x, p) = \langle \alpha | n \rangle \langle m | \alpha \rangle. \quad (\text{B3})$$

Because the target Hamiltonian is the liner superposition of $|n\rangle \langle m|$ with $n, m = 0, 1, \dots$, we just need to prove

$$\langle n' | H_{nm}(\hat{x}, \hat{p}) | m' \rangle = \delta_{n,n'} \delta_{m,m'}. \quad (\text{B4})$$

Using coherent state in the basis of Fock states $|\alpha\rangle = e^{-\frac{|\alpha|^2}{2}} \sum_n \frac{\alpha^n}{\sqrt{n!}} |n\rangle$, we calculate the Q-function of $|n\rangle\langle m|$

$$H_{nm}(x, p) = \langle \alpha | n \rangle \langle m | \alpha \rangle = \frac{1}{\sqrt{n!m!}} e^{-\frac{x^2+p^2}{2\lambda}} \left(\frac{x-ip}{\sqrt{2\lambda}} \right)^n \left(\frac{x+ip}{\sqrt{2\lambda}} \right)^m. \quad (\text{B5})$$

By introducing $x = r \cos \theta$, $p = r \sin \theta$ and $x = k \cos \tau$, $p = k \sin \tau$, we have the Fourier component

$$\begin{aligned} f_{nm}(k, \tau) &= \frac{e^{\frac{\lambda}{4}k^2}}{2\pi} \int \int r dr d\theta H_{nm}(r \cos \theta, r \sin \theta) e^{-ikr \cos(\theta-\tau)} \\ &= \frac{e^{i(m-n)\tau}}{\sqrt{n!m!}} \left(\frac{1}{\sqrt{2\lambda}} \right)^{m+n} \frac{e^{\frac{\lambda}{4}k^2}}{2\pi} \int_0^\infty r^{m+n+1} e^{-\frac{r^2}{2\lambda}} dr \int_0^{2\pi} d\theta e^{-ikr \cos(\theta-\tau) + i(m-n)(\theta-\tau)} \\ &= \frac{e^{i(m-n)\tau}}{\sqrt{n!m!}} \left(\frac{1}{\sqrt{2\lambda}} \right)^{m+n} e^{\frac{\lambda}{4}k^2} i^{n-m} \int_0^\infty r^{m+n+1} e^{-\frac{r^2}{2\lambda}} J_{n-m}(-kr) dr \\ &= e^{\frac{\lambda}{4}k^2} \sqrt{\frac{n!}{m!}} \left(i e^{i\tau} \frac{1}{k} \sqrt{\frac{2}{\lambda}} \right)^{m-n} \frac{\lambda}{\Gamma(1-m+n)} {}_1F_1(1+n; 1-m+n; -\frac{\lambda}{2}k^2) \end{aligned} \quad (\text{B6})$$

where $J_{n-m}(z)$ is the Bessel function with order of $n-m$, and ${}_1F_1(a; b; z)$ is the Kummer confluent hypergeometric function. We introduce the matrix element [84]

$$\langle n' | e^{i(k_x \hat{x} + k_p \hat{p})} | m' \rangle = e^{-\frac{\lambda}{4}(k_x^2 + k_p^2)} \left[\sqrt{\frac{\lambda}{2}} (k_p + ik_x) \right]^{m'-n'} \sqrt{\frac{n!}{m!}} L_{n'}^{m'-n'} \left[\frac{\lambda}{2} (k_x^2 + k_p^2) \right] \quad (\text{B7})$$

where $L_{n'}^{m'-n'}(z)$ is the generalized Laguerre polynomial. Then, we have the matrix element of $H_{nm}(\hat{x}, \hat{p})$ in Fock representation

$$\begin{aligned} \langle n' | H_{nm}(\hat{x}, \hat{p}) | m' \rangle &= \frac{1}{2\pi} \int \int dk_x dk_p f_{nm}(k_x, k_p) \langle n' | e^{i(k_x \hat{x} + k_p \hat{p})} | m' \rangle \\ &= e^{i\frac{\pi}{2}(m'-n')} \sqrt{\frac{n!}{m!}} \sqrt{\frac{n!}{m!}} \left(i \sqrt{\frac{2}{\lambda}} \right)^{m-n} \frac{\lambda}{\Gamma(1-m+n)} \\ &\quad \times \frac{1}{2\pi} \int_0^{2\pi} e^{i[(m-n)-(m'-n')]\tau} d\tau \\ &\quad \times \int_0^\infty dk \left(\sqrt{\frac{\lambda}{2}} k \right)^{m'-n'} k^{n-m+1} {}_1F_1(1+n; 1-m+n; -\frac{\lambda}{2}k^2) L_{n'}^{m'-n'} \left(\frac{\lambda}{2}k^2 \right) \\ &= \delta_{m-n, m'-n'} (-1)^{m-n} \sqrt{\frac{n!}{(m-n+n')!}} \sqrt{\frac{n!}{m!}} \frac{\lambda}{\Gamma(1-m+n)} \\ &\quad \times \int_0^\infty k dk {}_1F_1(1+n; 1-m+n; -\frac{\lambda}{2}k^2) L_{n'}^{m-n} \left(\frac{\lambda}{2}k^2 \right) \\ &= \delta_{m-n, m'-n'} (-1)^{m-n} \sqrt{\frac{n!}{(m-n+n')!}} \sqrt{\frac{n!}{m!}} \frac{2}{\Gamma(1-m+n)} \\ &\quad \times \int_0^\infty \tilde{k} d\tilde{k} {}_1F_1(1+n; 1-m+n; -\tilde{k}^2) L_{n'}^{m-n}(\tilde{k}^2) \quad (\text{where } \tilde{k} = \sqrt{\frac{\lambda}{2}}k) \\ &= \delta_{n, n'} \delta_{m, m'}. \end{aligned} \quad (\text{B8})$$

This is the identity (B4) we aim to prove. As a result, for a fixed λ , the mapping between Floquet Hamiltonians and Q-functions is one to one.

Note that the exponential suppression factor $e^{-\frac{\lambda}{4}(k_x^2 + k_p^2)}$ in Eq. (B7) cancels the same exponentially increasing factor in Eq. (B6). We will mention the sequence of this point in the discussion of sharp-boundary elliptical well below.

Appendix C: Designing driving potential

In this section, we show how to construct the driving potential from the NcFT coefficient such that its Floquet Hamiltonian equals to the target Hamiltonian in the leading order (RWA). We introduce the polar coordinate system

in (k_x, k_p) space via $(k_x = k \cos \tau, k_p = k \sin \tau)$, and write the Fourier expansion Eq. (A1) as

$$\hat{H}_F^{(T)} = \frac{1}{2\pi} \int_0^{2\pi} d\tau \int_{-\infty}^{+\infty} dk \frac{|k|}{2} f_T(k, \tau) e^{ik(\hat{x} \cos \tau + \hat{p} \sin \tau)}. \quad (\text{C1})$$

Here, we have defined the Fourier component in the polar coordinate system via $f_T(k, \tau) \equiv f_T(k_x, k_p)$, and allow for negative k via the relation $f_T(k, \tau) \equiv f_T^*(-k, \tau)$, cf. Eq.(A8). From the Fourier component of the target Hamiltonian $f_T(k, \tau)$, we design the real space driving potential as follows

$$V(x, t) = \int_{-\infty}^{+\infty} \frac{|k|}{2} f_T(k, \omega_0 t) e^{ikx} dk, \quad (\text{C2})$$

where the phase variable $\omega_0 t$ in time domain plays the role of angle τ in (k_x, k_p) space. By setting driving period $T_d = 2\pi/(\omega_0 q)$, the Hamiltonian in the rotating frame, cf. Eq. (3) in the main text, becomes

$$H(t) = \int_{-\infty}^{+\infty} \frac{1}{2} |k| f_T(k, \omega_0 t) e^{ik(\hat{x} \cos \omega_0 t + \hat{p} \sin \omega_0 t)} dk. \quad (\text{C3})$$

By time averaging the above Hamiltonian, cf. Eq. (4) in the main text, and comparing the averaged result to Eq. (C1), one can directly find that the lowest-order Floquet-Magnus expansion (RWA) gives the target Hamiltonian $H_F^{(T)}(\hat{x}, \hat{p})$. We can also write the engineered driving potential in real space as

$$V(x, t) = \int_0^{+\infty} |kf(k, \omega_0 t)| \cos[kx + \phi(k, t)] dk,$$

where we have introduced phase $\phi(k, t) = \text{Arg}[f_T(k, \omega_0 t)]$ and used the property $f(-k, \omega_0 t) = f^*(k, \omega_0 t)$. Thus, the driving potential can be engineered by superposing a series of cosine lattice potentials with tunable amplitudes $|kf_T(k, \omega_0 t)|$ and phases $\phi(k, t)$.

Appendix D: Rotational lattice Hamiltonian

We apply our method to engineer the target Floquet Hamiltonian with q -fold discrete rotational lattice symmetry in phase space

$$\hat{H}_{F\gamma}^{(T)} = \frac{\beta}{|\alpha_0|^{2q}} e^{-\gamma \hat{a}^\dagger \hat{a}} (\hat{a}^{\dagger q} - \alpha_0^{*q}) (\hat{a}^q - \alpha_0^q) e^{-\gamma \hat{a}^\dagger \hat{a}}, \quad (\text{D1})$$

where the factor $e^{-\gamma \hat{a}^\dagger \hat{a}}$ with $\gamma > 0$ is introduced to suppress the divergence of Hamiltonian in phase space. The above Hamiltonian is a generalised version of the rotational lattice Hamiltonian discussed in the main text, and it goes back to Eq. (9) by setting $\alpha_0 = 1/\sqrt{2\lambda}$. Using the identity

$$e^{-\gamma \hat{a}^\dagger \hat{a}} |\alpha\rangle = e^{-\frac{1}{2}(1-e^{-2\gamma})|\alpha|^2} |\alpha e^\gamma\rangle,$$

we have the Hamiltonian Q-function as follows

$$\begin{aligned} H_{Q\gamma}^{(T)}(x, p) &= \langle \alpha | \hat{H}_{F\gamma}^{(T)} | \alpha \rangle \\ &= \frac{\beta}{|\alpha_0 e^\gamma|^{2q}} \exp\left(-\frac{x^2 + p^2}{2\lambda\sigma_\gamma^2}\right) \left| \left(\frac{x + ip}{\sqrt{2\lambda}}\right)^q - \alpha_0^q e^{q\gamma} \right|^2. \end{aligned} \quad (\text{D2})$$

Here, we have defined the parameter $\sigma_\gamma = 1/\sqrt{1 - e^{-2\gamma}}$.

In order to obtain the analytical expression for the NcFT coefficient of Hamiltonian Q-function, we transform into the polar coordinate system by introducing $(x = r \cos \phi, p = r \sin \phi)$ and $(k_x = k \cos \tau, k_p = k \sin \tau)$. Plugging

Eq. (D2) into Eq. (A7), we have

$$\begin{aligned}
f_T(k, \tau) &= \frac{e^{\lambda k^2/4}}{2\pi\beta} \int_0^{+\infty} r dr \int_0^{2\pi} d\phi H_{Q\gamma}^{(T)}(r \cos \phi, r \sin \phi) e^{-ikr \cos(\phi-\tau)} \\
&= \frac{e^{\lambda k^2/4}}{|\alpha_0 e^\gamma|^{2q}} \int_0^{+\infty} r dr e^{-\frac{r^2}{2\lambda\sigma_\gamma^2}} \left[\frac{r^{2q}}{(2\lambda)^q} J_0(kr) - \frac{(ir\alpha_0 e^{\gamma-i\tau})^q}{(2\lambda)^{\frac{q}{2}}} J_{-q}(kr) - \frac{(-ir\alpha_0^* e^{\gamma+i\tau})^q}{(2\lambda)^{\frac{q}{2}}} J_q(kr) + |\alpha_0 e^\gamma|^{2q} J_0(kr) \right] \\
&= \frac{\lambda e^{\frac{\lambda}{4}k^2} \sigma_\gamma^{2(q+1)}}{|\alpha_0 e^\gamma|^{2q}} \left[n! {}_1F_1(1+q; 1; -\frac{\lambda}{2}\sigma_\gamma^2 k^2) - \left(-ie^{-i\tau} \alpha_0 e^\gamma \sqrt{\frac{\lambda}{2}} \right)^q k^q {}_1F_1(1+q; 1+q; -\frac{\lambda}{2}\sigma_\gamma^2 k^2) \right. \\
&\quad \left. - \left(-ie^{i\tau} \alpha_0^* e^\gamma \sqrt{\frac{\lambda}{2}} \right)^q k^q {}_1F_1(1+q; 1+q; -\frac{\lambda}{2}\sigma_\gamma^2 k^2) + \left| \frac{\alpha_0 e^\gamma}{\sigma_\gamma} \right|^{2q} {}_1F_1(1; 1; -\frac{\lambda}{2}\sigma_\gamma^2 k^2) \right]. \tag{D3}
\end{aligned}$$

Here, $J_q(\bullet)$ is the Bessel function of q -th order and ${}_1F_1(a; b; \bullet)$ is the Kummer confluent hypergeometric function.

In order to obtain an analytical expression for the driving potential $V(x, t)$, we introduce the following identities:

$$\begin{aligned}
\text{Identity I: } & \int_{-\infty}^{+\infty} \frac{1}{2} |k| e^{\frac{\lambda}{4}k^2} k^q {}_1F_1(1+q; 1+q; -\frac{\lambda}{2}\sigma_\gamma^2 k^2) e^{ikx} dk \\
&= 2^{q-1} (2\lambda\sigma_\gamma^2 - \lambda)^{-\frac{q+2}{2}} \left[q\Gamma\left(\frac{q}{2}\right) (1 + (-1)^q) {}_1F_1\left(\frac{q+2}{2}; \frac{1}{2}; -\frac{x^2}{2\lambda\sigma_\gamma^2 - \lambda}\right) \right. \\
&\quad \left. + 4ix(1 - (-1)^q) \Gamma\left(\frac{q+3}{2}\right) {}_1F_1\left(\frac{q+3}{2}; \frac{3}{2}; -\frac{x^2}{2\lambda\sigma_\gamma^2 - \lambda}\right) \right]; \tag{D4}
\end{aligned}$$

$$\text{Identity II: } \int_{-\infty}^{+\infty} \frac{1}{2} |k| e^{\frac{\lambda}{4}k^2} {}_1F_1(1; 1; -\frac{\lambda}{2}\sigma_\gamma^2 k^2) e^{ikx} dk = \frac{2}{2\lambda\sigma_\gamma^2 - \lambda} - \frac{4x}{(2\lambda\sigma_\gamma^2 - \lambda)^{\frac{3}{2}}} D\left(\frac{x}{\sqrt{2\lambda\sigma_\gamma^2 - \lambda}}\right); \tag{D5}$$

$$\begin{aligned}
\text{Identity III: } & \int_{-\infty}^{+\infty} \frac{1}{2} |k| e^{\frac{\lambda}{4}k^2} {}_1F_1(q+1; 1; -\frac{\lambda}{2}\sigma_\gamma^2 k^2) e^{ikx} dk \\
&= \int_0^{+\infty} k e^{\frac{\lambda}{4}k^2} {}_1F_1(q+1; 1; -\frac{\lambda}{2}\sigma_\gamma^2 k^2) \cos(kx) dk \\
&= \frac{1}{2} \sum_{m=0}^{+\infty} \frac{(-1)^m}{(2m)!} \int_0^{+\infty} e^{\frac{\lambda}{4}k^2} {}_1F_1(q+1; 1; -\frac{\lambda}{2}\sigma_\gamma^2 k^2) (kx)^{2m} dk^2 \\
&= \frac{1}{2} \sum_{m=0}^{+\infty} \frac{(-1)^m}{(2m)!} x^{2m} \int_0^{+\infty} e^{\frac{\lambda}{4}z} {}_1F_1(q+1; 1; -\frac{\lambda}{2}\sigma_\gamma^2 z) z^m dz \text{ (here, } z = k^2) \\
&= \frac{1}{2} \sum_{m=0}^{+\infty} \frac{(-1)^m}{(2m)!} x^{2m} \left(-\frac{4}{\lambda}\right)^{m+1} \Gamma(m+1) {}_2F_1(m+1, q+1; 1; 2\sigma_\gamma^2). \tag{D6}
\end{aligned}$$

Here, $\Gamma(\bullet)$ is the Gamma function and $D(z) = e^{-z^2} \int_0^z e^{t^2} dt$ is the Dawson function. Identity Eq. (D5) is the special case of identity Eq. (D4) by setting $n = 0$. In identity Eq. (D6), ${}_2F_1(a, b; c; z)$ is the hypergeometric function given by the path integral in the complex ζ -plane [85]

$${}_2F_1(a, b; c; z) = \frac{\Gamma(c)}{\Gamma(a)\Gamma(b)} \frac{1}{2\pi i} \int_{-i\infty}^{+i\infty} \frac{\Gamma(a+\zeta)\Gamma(b+\zeta)\Gamma(-\zeta)}{\Gamma(c+\zeta)} (-z)^\zeta d\zeta. \tag{D7}$$

The above integral is valid for $|\arg(-z)| \leq \pi - \epsilon$ ($0 < \epsilon < \pi$) and $a, b \notin \mathbb{Z}_0^-$. For $|z| < 1$, the hypergeometric function can be written by the power series

$${}_2F_1(a, b; c; z) = \sum_{k=0}^{\infty} \frac{(a)_k (b)_k}{(c)_k} \frac{z^k}{k!}, \quad |z| < 1 \tag{D8}$$

with the Pochhammer symbol $(x)_k = \Gamma(x+k)/\Gamma(x)$. The analytical continuation of ${}_2F_1(a, b; c; z)$ into the domain $|z| > 1$ can be realised from the following relationship [85]

$$\begin{aligned} {}_2F_1(a, b; c; z) &= \frac{\Gamma(c)\Gamma(b-a)}{\Gamma(b)\Gamma(c-a)} \left(-\frac{1}{z}\right)^a {}_2F_1(a, 1-c+a; 1-b+a; \frac{1}{z}) \\ &\quad + \frac{\Gamma(c)\Gamma(a-b)}{\Gamma(a)\Gamma(c-b)} \left(-\frac{1}{z}\right)^b {}_2F_1(b, 1-c+b; 1-a+b; \frac{1}{z}). \end{aligned} \quad (\text{D9})$$

The above relationship is valid for $|\arg(-z)| \leq \pi - \epsilon$ ($0 < \epsilon < \pi$) and $a - b \notin \mathbb{Z}$. From Eqs. (C2) and (D3)-(D6), we obtain the analytical expression for the designed driving potential for finite values of $\gamma > 0$ and arbitrary complex number α_0 as follows

$$\begin{aligned} V_\gamma(x, t) &= -\frac{(\lambda\sigma_\gamma^2)^{q+1}\Gamma(q+1)}{|\sqrt{\lambda}\alpha_0 e^\gamma|^{2q}} \sum_{m=0}^{+\infty} \frac{\Gamma(m+1)}{\Gamma(2m+1)} \frac{x^{2m}}{2} \left(\frac{4}{\lambda}\right)^{m+1} {}_2F_1(m+1, q+1; 1; 2\sigma_\gamma^2) \\ &\quad - \frac{(\lambda\sigma_\gamma^2)^{q+1}2^{q-1}}{|\sqrt{\lambda}\alpha_0 e^\gamma|^{2q}(2\lambda\sigma_\gamma^2 - \lambda)^{\frac{q+3}{2}}} \left[\left(-ie^{\gamma-i\tau}\alpha_0\sqrt{\frac{\lambda}{2}}\right)^q + \left(-ie^{\gamma+i\tau}\alpha_0^*\sqrt{\frac{\lambda}{2}}\right)^q \right] \\ &\quad \times \left[(1+(-1)^q)q\Gamma\left(\frac{q}{2}\right)\sqrt{2\lambda\sigma_\gamma^2 - \lambda} {}_1F_1\left(\frac{q+2}{2}; \frac{1}{2}; -\frac{x^2}{2\lambda\sigma_\gamma^2 - \lambda}\right) \right. \\ &\quad \left. + 4ix(1-(-1)^q)\Gamma\left(\frac{q+3}{2}\right) {}_1F_1\left(\frac{q+3}{2}; \frac{3}{2}; -\frac{x^2}{2\lambda\sigma_\gamma^2 - \lambda}\right) \right] \\ &\quad + \frac{2\sigma_\gamma^2}{2\sigma_\gamma^2 - 1} - \frac{1}{\sqrt{\lambda}} \frac{4x\sigma_\gamma^2}{(2\sigma_\gamma^2 - 1)^{\frac{3}{2}}} D\left(\frac{x}{\sqrt{2\lambda\sigma_\gamma^2 - \lambda}}\right). \end{aligned} \quad (\text{D10})$$

Next, we discuss how to calculate driving potential $V_\gamma(x, t)$ in the limit of $\gamma \rightarrow 0$ ($\sigma_\gamma = 1/\sqrt{1-e^{-2\gamma}} \rightarrow +\infty$). Using Eq. (D8), (D9) and the Euler's reflection formula $\Gamma(z)\Gamma(1-z) = \pi/\sin(\pi z)$, we obtain the following series expansion of the hypergeometric function for $|z| > 1$ and $q \in \mathbb{Z}_0^+$

$${}_2F_1(1+m, 1+q; 1; z) = \sum_{k=0}^{+\infty} \frac{\Gamma(m+k+1)^2(-1)^{m+q+1}}{\Gamma(1+m)\Gamma(1+q)\Gamma(m-q+k+1)} \frac{1}{k!} \left(\frac{1}{z}\right)^{k+m+1}. \quad (\text{D11})$$

Note that the parameter m actually can take the whole real values, i.e., $m \in \mathbb{R}$. Although the above expansion is not defined for m at negative integers $m \in \mathbb{Z}^-$, but the limit values do exist and can be defined as the values of the expansion for $m \in \mathbb{Z}^-$. By plugging the above series expansion Eq. (D11) and also the confluent hypergeometric function ${}_1F_1(a; b; z) = \sum_{k=0}^{+\infty} \frac{(a)_k}{(b)_k} \frac{z^k}{k!}$ into Eq. (D10), we obtain the driving potential in the limit of $\gamma \rightarrow 0$ ($\sigma_\gamma \rightarrow +\infty$)

$$V_{\gamma \rightarrow 0}(x, t) = \frac{1}{|\sqrt{\lambda}\alpha_0|^{2q}} \sum_{m=0}^{+\infty} \sum_{k=0}^{+\infty} \frac{2^{2m-q}\lambda^q x^{2m}}{\Gamma(2m+1)} \frac{\Gamma(m+k+1)^2(-1)^{m+q}}{\Gamma(m-q+k+1)} \frac{x^{2m}}{k!} \left(\frac{1}{2\sigma_\gamma^2}\right)^{k+m-q} \quad (\text{D12})$$

$$- \frac{1}{|\sqrt{\lambda}\alpha_0|^{2q}} \left[\left(-ie^{\gamma-i\tau}\alpha_0\sqrt{\frac{\lambda}{2}}\right)^q + \left(-ie^{\gamma+i\tau}\alpha_0^*\sqrt{\frac{\lambda}{2}}\right)^q \right] \quad (\text{D13})$$

$$\times \left[(1+(-1)^q) \sum_{m=0}^{+\infty} \frac{\Gamma(1+m+\frac{q}{2})\Gamma(\frac{1}{2})}{\Gamma(\frac{1}{2}+m)} (-1)^m 2^{\frac{q}{2}-m-1} (\lambda\sigma_\gamma^2)^{\frac{q}{2}-m} x^{2m} \right] \quad (\text{D14})$$

$$+ i(1-(-1)^q) \sum_{m=0}^{+\infty} \frac{\Gamma(\frac{3}{2}+m+\frac{q}{2})\Gamma(\frac{3}{2})}{\Gamma(\frac{3}{2}+m)} (-1)^m 2^{\frac{q}{2}-m-\frac{1}{2}} (\lambda\sigma_\gamma^2)^{\frac{q}{2}-m-\frac{1}{2}} x^{2m+1} \Big] \quad (\text{D15})$$

$$+ 1. \quad (\text{D16})$$

In line (D12), only terms that satisfy $k+m-q=0$ give nonzero contribution otherwise $\frac{1}{\Gamma(m+k-q+1)} \left(\frac{1}{2\sigma_\gamma^2}\right)^{k+m-q} = 0$ in the limit of $\sigma_\gamma = +\infty$ (note that Gamma function $\Gamma(z) = \infty$ for nonpositive integer argument $z \in \mathbb{Z}_0^-$). In line (D14), only terms with even integer q and $m \leq q/2$ give nonzero contribution. Furthermore, we emphasise that the driving potential $V(x, t)$ is obtained from the RWA. In the rotating frame, the oscillating terms from $m < q/2$ cannot cancel the time-dependent parts given by terms that contain $e^{\pm iq\tau}$ in line (D13). Therefore, the only nontrivial contribution

comes from the term with $m = q/2$ in line (D14). For the same reason, only nontrivial contribution comes from the term with $m = (q - 1)/2$ in line (D15). By neglecting these terms, we have the designed driving potential

$$\begin{aligned}
V(x, t) &= \frac{1}{|\sqrt{2\lambda}\alpha_0|^{2q}} \sum_{m=0}^q (-1)^{m+q} \frac{(2^m q!)^2}{(2m)!(q-m)!} \lambda^{q-m} x^{2m} \\
&\quad - \frac{(-i)^q}{|\sqrt{2\lambda}\alpha_0|^{2q}} \left[\left(e^{-i\tau} \alpha_0 \sqrt{2\lambda} \right)^q + \left(e^{i\tau} \alpha_0^* \sqrt{2\lambda} \right)^q \right] \\
&\quad \times \left([1 + (-1)^q] \frac{\Gamma(1+q)\Gamma(\frac{1}{2})}{\Gamma(\frac{1}{2} + \frac{q}{2})} \frac{(-1)^{\frac{q}{2}}}{2} + i[1 - (-1)^q] \frac{\Gamma(q+1)\Gamma(\frac{3}{2})}{\Gamma(\frac{q}{2} + 1)} (-1)^{\frac{q-1}{2}} \right) x^q \\
&\quad + 1.
\end{aligned} \tag{D17}$$

By taking the value of $\alpha_0 = 1/\sqrt{2\lambda}$, we obtain the driving potential given by Eq. (10) shown in the main text, i.e.,

$$\begin{aligned}
V(x, t) &= \sum_{m=0}^q \frac{(2^m q!)^2 (-1)^{q+m}}{(2m)!(q-m)!} \lambda^{q-m} x^{2m} - \sqrt{\pi} q! \left[\frac{1 + (-1)^q}{\Gamma(\frac{q}{2} + \frac{1}{2})} + \frac{1 - (-1)^q}{\Gamma(\frac{q}{2} + 1)} \right] \cos(q\tau) x^q + 1 \\
&= \sum_{m=0}^q B_{q,m} \lambda^{q-m} x^{2m} - C_q \cos(q\omega_0 t) x^q + 1.
\end{aligned} \tag{D18}$$

Here, we have defined the coefficients $B_{q,m} = \frac{(2^m q!)^2 (-1)^{q+m}}{(2m)!(q-m)!}$ and $C_q = \sqrt{\pi} q! \left[\frac{1 + (-1)^q}{\Gamma(\frac{q}{2} + \frac{1}{2})} + \frac{1 - (-1)^q}{\Gamma(\frac{q}{2} + 1)} \right] = \frac{2\sqrt{\pi} q!}{\Gamma((2q+3-(-1)^q)/4)}$.

Appendix E: Ground state property of rotational lattice Hamiltonian

In the main text, we have claimed that the groundstate manifold of present rotational lattice Hamiltonian is q -dimensional and is spanned by q q -legged cat states. This is because the q coherent states $|\alpha_m\rangle = |e^{im\frac{2\pi}{q}}/\sqrt{2\lambda}\rangle$ with $m = 0, 1, \dots, q-1$ are exact zero-energy eigenstates and quantum fluctuations do not introduce any tunneling between these coherent states. Mathematically, the q -fold symmetry of Hamiltonian in phase space is described by

$$\hat{R}_q \hat{H}_F^{(T)} \hat{R}_q^\dagger = \hat{H}_F^{(T)}, \tag{E1}$$

where $\hat{R}_q \equiv e^{i\hat{a}^\dagger \hat{a} \frac{2\pi}{q}}$ is the discrete rotational operation [20, 36]. According to the Bloch theorem extended in phase space [36], the eigensates of Hamiltonian can be written in form of

$$|\psi_{l,m}\rangle = \frac{1}{\sqrt{q}} \sum_{p=0}^{q-1} e^{imp\frac{2\pi}{q}} \hat{R}_q^p |\phi_l\rangle, \tag{E2}$$

where index l labels the Bloch bands, m is called quasinumber and $|\phi_l\rangle$ is the Wannier state of l -th Bloch band. The Wannier state $|\phi_l\rangle$ for the lowest band can be chosen by the coherent state $|\alpha_0\rangle$, and the constructed Bloch states are exact eigenstates that are exactly degenerate (flat band). The single-photon loss only alternates the Bloch eigenstates inside the band:

$$\begin{aligned}
\hat{a}|\psi_{l,m}\rangle &= \frac{1}{\sqrt{q}} \sum_{p=0}^{q-1} e^{imp\frac{2\pi}{q}} \hat{a} \hat{R}_q^p |\alpha_0\rangle \\
&= \frac{1}{\sqrt{q}} \sum_{p=0}^{q-1} e^{imp\frac{2\pi}{q}} \hat{R}_q^p \hat{R}_q^\dagger \hat{a} \hat{R}_q^p |\alpha_0\rangle \\
&= \frac{\alpha_0}{\sqrt{q}} \sum_{p=0}^{q-1} e^{i(m-1)p\frac{2\pi}{q}} \hat{R}_q^p |\alpha_0\rangle \\
&\propto |\psi_{l,m-1}\rangle.
\end{aligned} \tag{E3}$$

In the third line, we have used the property $\hat{R}_q^\dagger \hat{a} \hat{R}_q = \hat{a} e^{-i\frac{2\pi}{q}}$ and $\hat{a}|\alpha_0\rangle = \alpha_0|\alpha_0\rangle$. Thus, photon decay does not leak quantum information out of the code subspaces [16, 28–30], allowing for fault tolerant syndrome detection that exponentially suppresses phase flips and does not cause error backaction on the encoded system [28].

Appendix F: Sharp-boundary elliptical well in phase space

In this section, we calculate analytical expression of the engineered driving potential for the elliptical Hamiltonian in phase space. We start from the general formula of the engineered driving potential as follows

$$V(x, t) = \frac{1}{2} \int_{-\infty}^{+\infty} |k| f_T(k, t) e^{ikx} dk. \quad (\text{F1})$$

According to the identity $x^{-2} = -\frac{1}{2} \int_{-\infty}^{+\infty} |k| e^{ikx} dk$ and defining the following function

$$v(x, t) \equiv \frac{1}{2\pi} \int_{-\infty}^{+\infty} f_T(k, t) e^{ikx} dk, \quad (\text{F2})$$

the driving potential $V(x, t)$ is the convolution of $-x^{-2}$ and $u(x, t)$, i.e.,

$$\begin{aligned} V(x, t) &= -x^{-2} * v(x, t) \\ &= - \int_{-\infty}^{+\infty} \frac{1}{z^2} v(x-z, t) dz \\ &= - \lim_{\epsilon \rightarrow 0^+} \int_{-\infty}^{+\infty} \Re \left[\frac{1}{(z-i\epsilon)^2} \right] v(x-z, t) dz \\ &= - \lim_{\epsilon \rightarrow 0^+} \int_{-\infty}^{+\infty} \frac{z^2 - \epsilon^2}{(z^2 + \epsilon^2)^2} v(x-z, t) dz. \end{aligned} \quad (\text{F3})$$

Here, we should first replace the convolution function $1/z^2$ by $(z^2 - \epsilon^2)/(z^2 + \epsilon^2)^2$ to get converged integral, and then take the limit of $\epsilon \rightarrow 0$ to obtain $V(x, t)$.

In the (x, p) phase space, we set a new coordinate (x', p') system which is rotated by an angle τ between x and x' axes given by the following orthogonal transformation

$$x = x' \cos \tau - p' \sin \tau; \quad p = x' \sin \tau + p' \cos \tau. \quad (\text{F4})$$

We can express the target Hamiltonian Q-function with rotated coordinates by $H_Q'^{(T)}(x', p') \equiv H_Q^{(T)}(x, p)$. Then, we project the Hamiltonian on the x' axis by the so-called *Radon transformation*

$$\mathcal{R}_\tau[H_Q'^{(T)}](x') = \int_{-\infty}^{+\infty} H_Q'^{(T)}(x', p') dp'. \quad (\text{F5})$$

The 1D Fourier transformation of the above projected function is given by

$$\mathcal{F}[\mathcal{R}_\tau[H_Q'^{(T)}]](k_{x'}) = \int \mathcal{R}_\tau[H_Q'^{(T)}](x') e^{-ik_{x'} x'} dx'. \quad (\text{F6})$$

The 2D Fourier transformation of $H_Q'^{(T)}(x', p')$ is

$$\mathcal{F}[H_Q'^{(T)}](k_{x'}, k_{p'}) = \int \int H_Q'^{(T)}(x', p') e^{-i(k_{x'} x' + k_{p'} p')} dx' dp'. \quad (\text{F7})$$

By plugging Eq. (F5) into Eq. (F6) and comparing with Eq. (F7), we have

$$\mathcal{F}[\mathcal{R}_\tau[H_Q'^{(T)}]](k_{x'}) = \mathcal{F}[H_Q'^{(T)}](k_{x'}, k_{p'} = 0). \quad (\text{F8})$$

This is the so-called projection-slice theorem [86, 87]. Comparing to Eq. (A7) and using the orthogonal transformation (F4), we have $\mathcal{F}[\mathcal{R}_\tau[H_Q'^{(T)}]](k) = 2\pi f_T(k, \tau) e^{-\frac{\lambda}{4} k^2}$ (here we have set $k_{x'} = k$) and thus

$$\mathcal{R}_\tau[H_Q'^{(T)}](x) = \int_{-\infty}^{+\infty} f_T(k, \tau) e^{-\frac{\lambda}{4} k^2} e^{ikx} dk. \quad (\text{F9})$$

In the classical limit $\lambda = 0$, according to Eqs. (F2) and (F3), we have $v(x, \tau) = \frac{1}{2\pi} \mathcal{R}_\tau[H_Q^{(T)}](x)$ and thus

$$V(x, t) = -\frac{1}{2\pi} \frac{1}{x^2} * \mathcal{R}_{\tau=t}[H_Q^{(T)}](x). \quad (\text{F10})$$

Now, we apply the convolutional form (F3) and Radon transformation (F5) to calculate the engineered driving potential for the elliptical well in phase space in the classical limit $\lambda = 0$. The boundary of the elliptical Hamiltonian Q-function in phase space is given by

$$\frac{(x' \cos \tau - p' \sin \tau)^2}{a^2} + \frac{(x' \sin \tau + p' \cos \tau)^2}{b^2} = 1.$$

Using the transformation (F4), we have the following

$$\left(\frac{\sin^2 \tau}{a^2} + \frac{\cos^2 \tau}{b^2}\right) p'^2 - \sin(2\tau) \left(\frac{1}{a^2} - \frac{1}{b^2}\right) x' p' + \left(\frac{\cos^2 \tau}{a^2} + \frac{\sin^2 \tau}{b^2}\right) x'^2 - 1 = 0.$$

Using the two solutions p'_1 and p'_2 of the above equation, the length across the ellipse is

$$\begin{aligned} |p'_1 - p'_2| &= \sqrt{(p'_1 + p'_2)^2 - 4p'_1 p'_2} \\ &= \sqrt{\frac{1}{A^2} x'^2 \sin^2 2\tau \left(\frac{1}{a^2} - \frac{1}{b^2}\right)^2 - \frac{4}{A} \left[x'^2 \left(\frac{\cos^2 \tau}{a^2} + \frac{\sin^2 \tau}{b^2}\right) - 1\right]} \\ &= \frac{2}{\sqrt{A}} \sqrt{1 - Bx'^2} \end{aligned} \quad (\text{F11})$$

where

$$A(\tau) \equiv \frac{\sin^2 \tau}{a^2} + \frac{\cos^2 \tau}{b^2}, \quad B(\tau) \equiv \left(\frac{\cos^2 \tau}{a^2} + \frac{\sin^2 \tau}{b^2}\right) - \frac{1}{4A(\tau)} \sin^2 2\tau \left(\frac{1}{a^2} - \frac{1}{b^2}\right)^2 \quad (\text{F12})$$

From Eq. (F5), we have the Radon transformation

$$\mathcal{R}_\tau[H_Q^{(T)}](x') = -|p'_1 - p'_2| = -\frac{2}{\sqrt{A(\tau)}} \sqrt{1 - B(\tau)x'^2} \quad \text{for } |x'| < \frac{1}{\sqrt{B(\tau)}}. \quad (\text{F13})$$

From Eq. (F10), the driving potential is given by

$$\begin{aligned} V(x, t) &= -\frac{1}{2\pi} x^{-2} * \mathcal{R}_t[H_Q^{(T)}](x) \\ &= -\frac{1}{2\pi} \lim_{\epsilon \rightarrow 0^+} \int_{-\infty}^{+\infty} \frac{z^2 - \epsilon^2}{(z^2 + \epsilon^2)^2} \mathcal{R}_t[H_Q^{(T)}](x - z) dz \\ &= \frac{1}{2\pi} 2\sqrt{\frac{B}{A}} \lim_{\epsilon \rightarrow 0^+} \int_{-\infty}^{+\infty} \frac{z^2 - \epsilon^2}{(z^2 + \epsilon^2)^2} \sqrt{\left(\frac{1}{\sqrt{B}} - x + z\right) \left(\frac{1}{\sqrt{B}} + x - z\right)} dz \\ &= -\sqrt{\frac{B}{A}} \lim_{\epsilon \rightarrow 0^+} \left(1 - \Re\left[\frac{\epsilon - ix}{\sqrt{B^{-1} + (\epsilon - ix)^2}}\right]\right) \end{aligned} \quad (\text{F14})$$

In the limit $\epsilon = 0$, we have

$$V(x, t) = \begin{cases} -\sqrt{\frac{B(t)}{A(t)}}, & |x| < \frac{1}{\sqrt{B(t)}} \\ -\sqrt{\frac{B(t)}{A(t)}} \left(1 - \frac{|x|}{\sqrt{x^2 - \frac{1}{B(t)}}}\right), & |x| \geq \frac{1}{\sqrt{B(t)}}. \end{cases} \quad (\text{F15})$$

This is the driving potential that can generate classical elliptical potential with sharp boundary in phase space.

Note that the value of $V(x, t)$ is divergent at $x = \pm 1/\sqrt{B(t)}$ according to Eq. (F15). In fact, the Fourier coefficient Eq. (A7) is always divergent for $k \rightarrow \infty$ in the quantum regime $\lambda > 0$. For physical result, we can add an exponentially suppressing factor to the Fourier coefficient:

$$f_T(k_x, k_p) \rightarrow f_T(k_x, k_p) e^{-\frac{1}{2}\sigma^2(k_x^2 + k_p^2)} \quad \text{with } \sigma > \sqrt{\lambda/2}. \quad (\text{F16})$$

According to the convolution theorem [88], we equivalently modify the Hamiltonian Q-function with a convolution operation, i.e.,

$$H_{Q,\sigma}^{(T)} = \int \int dx' dp' g(x', p') H_Q^{(T)}(x - x', p - p') \quad \text{with} \quad g(x, p) = \frac{1}{2\pi\sigma^2} e^{-\frac{x^2+p^2}{2\sigma^2}}. \quad (\text{F17})$$

The kernel function $g(x, p)$ smooths the sharp boundary of the elliptical well. Correspondingly, the driving potential is also modified with a convolution, i.e.,

$$V_\sigma(x, t) = \int dx' h(x') V(x - x', t) \quad \text{with} \quad h(x) = \frac{1}{\sqrt{\pi(2\sigma^2 - \lambda)}} e^{-\frac{x^2}{2\sigma^2 - \lambda}}. \quad (\text{F18})$$

We point out that, in the Fock representation, the exponential suppression factor $e^{-\frac{\lambda}{4}(k_x^2+k_p^2)}$ in Eq. (B7) cancels the same exponentially increasing factor in Eq. (B6). As a result, a sharp well with boundary narrower than quantum fluctuations ($\sigma < \sqrt{\lambda/2}$) does exist. However, this scenario cannot be realised by our present method.

Appendix G: Moiré superlattice

In this section, we discuss how to engineer a Moiré superlattice in phase space that is formed by two honeycomb phase space lattices overlaid with a relative twist angle and confined in a finite region with radius R ,

$$H_Q^{(T)}(x, p) = \begin{cases} H_{\theta=0} + H_{\theta=\theta_0}, & \sqrt{x^2 + p^2} \leq R \\ 0, & \sqrt{x^2 + p^2} > R. \end{cases} \quad (\text{G1})$$

Here, $H_\theta(x, p) \equiv -\prod_{n=1}^3 \sin^2[\frac{1}{2}\mathbf{v}_n \cdot \mathbf{z}(\theta)] + \frac{3}{32}$ is the honeycomb lattice in phase space [40]. We have defined the vector $\mathbf{z}(\theta) \equiv (x \cos \theta + p \sin \theta, -x \sin \theta + p \cos \theta)$, and three ancillary vectors

$$\mathbf{v}_1 = (\frac{2\sqrt{3}}{3}, 0), \quad \mathbf{v}_2 = (-\frac{\sqrt{3}}{3}, 1), \quad \mathbf{v}_3 = (-\frac{\sqrt{3}}{3}, -1). \quad (\text{G2})$$

In Fig. 3(a) in the main text, we plot the resulting Moiré superlattice Q-function with twisted angle $\theta_0 = 10^\circ$.

We calculate and plot the NcFT coefficient $f_T(k_x, k_p)$ in Fig. 3(b) in the main text, which composes of discrete peaks reflecting the discrete translational symmetry of target Hamiltonian in phase space. The centers of these peaks take place at $(k_x^q = k_q \cos \tau_q, k_p^q = k_q \sin \tau_q)$ where $\tau_q = q\pi/6, q\pi/6 + \theta_0$ and $k_q = 2/\sqrt{3}, 2, 4/\sqrt{3}$ with $q \in \mathbb{Z}$. The finite width of peaks comes from the boundary condition of Moiré superlattice. In fact, we have the analytical expression from Eq. (A7)

$$f_T(k_x, k_p) = \sum_q \frac{A_q}{2\pi} \frac{J_1\left(R\sqrt{(k_x - k_x^q)^2 + (k_p - k_p^q)^2}\right)}{R^{-1}\sqrt{(k_x - k_x^q)^2 + (k_p - k_p^q)^2}}, \quad (\text{G3})$$

where $A_q = \pi/16, -\pi/16, \pi/32$ for $k_q = 2\sqrt{3}, 2, 4\sqrt{3}$ respectively. Due to the long-distance asymptotic behavior of Bessel function

$$J_1(k) \approx \sqrt{\frac{2}{\pi k}} \cos\left(k - \frac{\pi}{4}\right) \quad \text{for} \quad |k| \gg 1, \quad (\text{G4})$$

we have added an exponentially suppressing factor $e^{-\frac{\lambda}{4}(k_x^2+k_p^2)}$ to obtain convergent NcFT coefficient. As a result, the Hamiltonian Q-function smoothed with a convolution kernel function $g(x, p) = \frac{1}{\pi\lambda} e^{-\frac{x^2+p^2}{\lambda}}$, cf. Eq. (F17).

Appendix H: Hamiltonian operator and Q-function symmetry

In this section, we prove that the Hamiltonian operator and its Q-function has the same symmetry in phase space. We first discuss the Hamiltonian operator in the discrete rotational operation $\hat{R}_q \equiv e^{i\hat{a}^\dagger \hat{a} \frac{2\pi}{q}}$. From the Fourier form

of Hamiltonian operator Eq. (A1), we have

$$\begin{aligned}
\hat{R}_q H(\hat{x}, \hat{p}) \hat{R}_q^\dagger &= \frac{\beta}{2\pi} \int \int dk_x dk_p f_T(k_x, k_p) \hat{R}_q \exp[i(k_x \hat{x} + k_p \hat{p})] \hat{R}_q^\dagger \\
&= \frac{\beta}{2\pi} \int \int dk_x dk_p f_T(k_x, k_p) \exp \left[i \left[\left(k_x \cos\left(\frac{2\pi}{q}\right) - k_p \sin\left(\frac{2\pi}{q}\right) \right) \hat{x} + \left(k_x \sin\left(\frac{2\pi}{q}\right) + k_p \cos\left(\frac{2\pi}{q}\right) \right) \hat{p} \right] \right] \\
&= \frac{\beta}{2\pi} \int \int dk'_x dk'_p f_T(k'_x, k'_p) \exp[i(k'_x \hat{x} + k'_p \hat{p})].
\end{aligned} \tag{H1}$$

Here, we have used the property

$$\begin{cases} \hat{R}_q \hat{x} \hat{R}_q^\dagger = \hat{x} \cos\left(\frac{2\pi}{q}\right) + \hat{p} \sin\left(\frac{2\pi}{q}\right) \\ \hat{R}_q \hat{p} \hat{R}_q^\dagger = -\hat{x} \sin\left(\frac{2\pi}{q}\right) + \hat{p} \cos\left(\frac{2\pi}{q}\right), \end{cases} \tag{H2}$$

and transformed the integral coordinates by

$$\begin{cases} k'_x = k_x \cos\left(\frac{2\pi}{q}\right) - k_p \sin\left(\frac{2\pi}{q}\right) \\ k'_p = k_x \sin\left(\frac{2\pi}{q}\right) + k_p \cos\left(\frac{2\pi}{q}\right) \end{cases} \tag{H3}$$

with the property $dk_x dk_p = dk'_x dk'_p$ as the transformation is orthogonal.

Next, we will prove the NcFT coefficient of rotational lattice satisfies $f(k'_x, k'_p) = f(k_x, k_p)$. According to (A7), we have

$$\begin{aligned}
f_T(k'_x, k'_p) &= \frac{e^{\frac{\lambda}{4}(k'^2_x + k'^2_p)}}{2\pi\beta} \int \int dx dp H_Q^{(T)}(x, p) e^{-i(k'_x x + k'_p p)} \\
&= \frac{e^{\frac{\lambda}{4}(k^2_x + k^2_p)}}{2\pi\beta} \int \int dx' dp' H_Q^{(T)}(x', p') e^{-i(k_x x' + k_p p')},
\end{aligned} \tag{H4}$$

where we have used transformation Eq. (H3) and made the orthogonal transformation in the phase space plane

$$\begin{cases} x' = x \cos\left(\frac{2\pi}{q}\right) + p \sin\left(\frac{2\pi}{q}\right) \\ p' = -x \sin\left(\frac{2\pi}{q}\right) + p \cos\left(\frac{2\pi}{q}\right). \end{cases} \tag{H5}$$

Therefore, if the Hamiltonian Q-function satisfied the discrete rotational symmetry $H_Q^{(T)}(x', p') = H_Q^{(T)}(x, p)$, the NcFT coefficient of rotational lattice satisfies $f(k_x, k_p) = f(k'_x, k'_p)$. Then, comparing Eq. (A1) and Eq. (H1), we have $\hat{R}_q H(\hat{x}, \hat{p}) \hat{R}_q^\dagger = H(\hat{x}, \hat{p})$ and vice versa .

The same discussion can also be applied for the translational symmetry described by the displacement operator

$$\begin{aligned}
\hat{D}_{\alpha_0} H(\hat{x}, \hat{p}) \hat{D}_{\alpha_0}^\dagger &= \frac{\beta}{2\pi} \int \int dk_x dk_p f_T(k_x, k_p) \hat{D}_{\alpha_0} \exp[i(k_x \hat{x} + k_p \hat{p})] \hat{D}_{\alpha_0}^\dagger \\
&= \frac{\beta}{2\pi} \int \int dk_x dk_p f_T(k_x, k_p) e^{-i(k_x x_0 + k_p p_0)} \exp[i(k_x \hat{x} + k_p \hat{p})],
\end{aligned} \tag{H6}$$

where we have used the property $\hat{D}_{\alpha_0} \hat{a} \hat{D}_{\alpha_0}^\dagger = \hat{a} - \alpha_0$ and thus

$$\begin{cases} \hat{D}_{\alpha_0} \hat{x} \hat{D}_{\alpha_0}^\dagger = \hat{x} - x_0 \text{ with } x_0 = \langle \alpha_0 | \hat{x} | \alpha_0 \rangle \\ \hat{D}_{\alpha_0} \hat{p} \hat{D}_{\alpha_0}^\dagger = \hat{p} - p_0 \text{ with } p_0 = \langle \alpha_0 | \hat{p} | \alpha_0 \rangle. \end{cases} \tag{H7}$$

From Eq. (A7), we have

$$\begin{aligned}
f_T(k_x, k_p) e^{-i(k_x x_0 + k_p p_0)} &= \frac{e^{\frac{\lambda}{4}(k^2_x + k^2_p)}}{2\pi\beta} \int \int dx dp H_Q^{(T)}(x, p) e^{-i[k_x(x+x_0) + k_p(p+p_0)]} \\
&= \frac{e^{\frac{\lambda}{4}(k^2_x + k^2_p)}}{2\pi\beta} \int \int dx dp H_Q^{(T)}(x+x_0, p+p_0) e^{-i(k_x x + k_p p)}.
\end{aligned} \tag{H8}$$

Therefore, if the Hamiltonian Q-function satisfied the translational symmetry $H_Q^{(T)}(x+x_0, p+p_0) = H_Q^{(T)}(x, p)$, the NcFT coefficient of rotational lattice satisfies $f_T(k_x, k_p) e^{-i(k_x x_0 + k_p p_0)} = f(k_x, k_p)$. Then, comparing Eq. (A1) and Eq. (H6), we have $\hat{D}_{\alpha_0} H(\hat{x}, \hat{p}) \hat{D}_{\alpha_0}^\dagger = H(\hat{x}, \hat{p})$ and vice versa .

The same discussion can also be applied for other phase-space symmetries like the mirror symmetry, i.e., if the Hamiltonian Q-function satisfies $H_Q^{(T)}(x_0, p) = H_Q^{(T)}(\pm x, \pm p)$, the Hamiltonian operator has $H(\pm\hat{x}, \pm\hat{p}) = H(\pm\hat{x}, \pm\hat{p})$ and vice versa.

Lastly, we point out that the conclusion is also true for the smoothed Hamiltonian Q-function with a convolution operation, i.e.,

$$H_{Q,\sigma}^{(T)} = \int \int dx' dp' g(x', p') H_Q^{(T)}(x - x', p - p') \quad (\text{H9})$$

as long as the kernel function is rotationally symmetric, e.g., the standard Gaussian kernel $g(x, p) = \frac{1}{2\pi\sigma^2} \exp(-\frac{x^2+p^2}{2\sigma^2})$.

-
- [1] C. Gerry and P. Knight, *Nonclassical light* (Cambridge University Press, Cambridge, 2004), pp. 150–194, Introductory Quantum Optics, ISBN 9780521527354.
- [2] D. V. Strekalov and G. Leuchs, *Nonlinear Interactions and Non-classical Light* (Springer International Publishing, Cham, 2019), pp. 51–101, ISBN 978-3-319-98402-5.
- [3] B. Kubala, V. Gramich, and J. Ankerhold, *Physica Scripta* **T165**, 014029 (2015), URL <https://doi.org/10.1088/0031-8949/2015/t165/014029>.
- [4] S. L. Braunstein and P. van Loock, *Rev. Mod. Phys.* **77**, 513 (2005), URL <https://link.aps.org/doi/10.1103/RevModPhys.77.513>.
- [5] J.-W. Pan, Z.-B. Chen, C.-Y. Lu, H. Weinfurter, A. Zeilinger, and M. Żukowski, *Rev. Mod. Phys.* **84**, 777 (2012), URL <https://link.aps.org/doi/10.1103/RevModPhys.84.777>.
- [6] Z.-H. Yan, J.-L. Qin, Z.-Z. Qin, X.-L. Su, X.-J. Jia, C.-D. Xie, and K.-C. Peng, *Fundamental Research* **1**, 43 (2021), ISSN 2667-3258, URL <https://www.sciencedirect.com/science/article/pii/S2667325820300054>.
- [7] Z. Leghtas, G. Kirchmair, B. Vlastakis, R. J. Schoelkopf, M. H. Devoret, and M. Mirrahimi, *Phys. Rev. Lett.* **111**, 120501 (2013), URL <https://link.aps.org/doi/10.1103/PhysRevLett.111.120501>.
- [8] M. Mirrahimi, Z. Leghtas, V. V. Albert, S. Touzard, R. J. Schoelkopf, L. Jiang, and M. H. Devoret, *New Journal of Physics* **16**, 045014 (2014), URL <https://doi.org/10.1088/1367-2630/16/4/045014>.
- [9] R. W. Heeres, P. Reinhold, N. Ofek, L. Frunzio, L. Jiang, M. H. Devoret, and R. J. Schoelkopf, *Nature Communications* **8**, 94 (2017), ISSN 2041-1723, URL <https://doi.org/10.1038/s41467-017-00045-1>.
- [10] S. Rosenblum, P. Reinhold, M. Mirrahimi, L. Jiang, L. Frunzio, and R. J. Schoelkopf, *Science* **361**, 266 (2018), <https://www.science.org/doi/pdf/10.1126/science.aat3996>, URL <https://www.science.org/doi/abs/10.1126/science.aat3996>.
- [11] C. Flühmann, T. L. Nguyen, M. Marinelli, V. Negnevitsky, K. Mehta, and J. P. Home, *Nature* **566**, 513 (2019), ISSN 1476-4687, URL <https://doi.org/10.1038/s41586-019-0960-6>.
- [12] L. Hu, Y. Ma, W. Cai, X. Mu, Y. Xu, W. Wang, Y. Wu, H. Wang, Y. P. Song, C.-L. Zou, et al., *Nature Physics* **15**, 503 (2019), ISSN 1745-2481, URL <https://doi.org/10.1038/s41567-018-0414-3>.
- [13] P. Campagne-Ibarcq, A. Eickbusch, S. Touzard, E. Zalsgeller, N. E. Frattini, V. V. Sivak, P. Reinhold, S. Puri, S. Shankar, R. J. Schoelkopf, et al., *Nature* **584**, 368 (2020), ISSN 1476-4687, URL <https://doi.org/10.1038/s41586-020-2603-3>.
- [14] J. M. Gertler, B. Baker, J. Li, S. Shirol, J. Koch, and C. Wang, *Nature* **590**, 243 (2021), ISSN 1476-4687, URL <https://doi.org/10.1038/s41586-021-03257-0>.
- [15] P. T. Cochrane, G. J. Milburn, and W. J. Munro, *Phys. Rev. A* **59**, 2631 (1999), URL <https://link.aps.org/doi/10.1103/PhysRevA.59.2631>.
- [16] D. Gottesman, A. Kitaev, and J. Preskill, *Phys. Rev. A* **64**, 012310 (2001), URL <https://link.aps.org/doi/10.1103/PhysRevA.64.012310>.
- [17] B. C. Travaglione and G. J. Milburn, *Phys. Rev. A* **66**, 052322 (2002), URL <https://link.aps.org/doi/10.1103/PhysRevA.66.052322>.
- [18] M. H. Michael, M. Silveri, R. T. Brierley, V. V. Albert, J. Salmilehto, L. Jiang, and S. M. Girvin, *Phys. Rev. X* **6**, 031006 (2016), URL <https://link.aps.org/doi/10.1103/PhysRevX.6.031006>.
- [19] V. V. Albert, K. Noh, K. Duivenvoorden, D. J. Young, R. T. Brierley, P. Reinhold, C. Vuillot, L. Li, C. Shen, S. M. Girvin, et al., *Phys. Rev. A* **97**, 032346 (2018), URL <https://link.aps.org/doi/10.1103/PhysRevA.97.032346>.
- [20] A. L. Grimsmo, J. Combes, and B. Q. Baragiola, *Phys. Rev. X* **10**, 011058 (2020), URL <https://link.aps.org/doi/10.1103/PhysRevX.10.011058>.
- [21] I. Tzitrin, J. E. Bourassa, N. C. Menicucci, and K. K. Sabapathy, *Phys. Rev. A* **101**, 032315 (2020), URL <https://link.aps.org/doi/10.1103/PhysRevA.101.032315>.
- [22] B. M. Terhal, J. Conrad, and C. Vuillot, *Quantum Science and Technology* **5**, 043001 (2020), URL <https://doi.org/10.1088/2058-9565/ab98a5>.
- [23] A. Joshi, K. Noh, and Y. Y. Gao, *Quantum Science and Technology* **6**, 033001 (2021), URL <https://doi.org/10.1088/2058-9565/abe989>.
- [24] W. Cai, Y. Ma, W. Wang, C.-L. Zou, and L. Sun, *Fundamental Research* **1**, 50 (2021), ISSN 2667-3258, URL <https://www.sciencedirect.com/science/article/pii/S2667325820300145>.
- [25] S. Krastanov, V. V. Albert, C. Shen, C.-L. Zou, R. W. Heeres, B. Vlastakis, R. J. Schoelkopf, and L. Jiang, *Phys. Rev. A* **92**, 040303 (2015), URL <https://link.aps.org/doi/10.1103/PhysRevA.92.040303>.
- [26] T. Fösel, S. Krastanov, F. Marquardt, and L. Jiang, *Efficient cavity control with snap gates* (2020), URL <https://arxiv.org/abs/2004.14256>.
- [27] M. Kudra, M. Kervinen, I. Strandberg, S. Ahmed, M. Scigliuzzo, A. Osman, D. P. Lozano, M. O. Tholén, R. Borgani, D. B. Haviland, et al., *PRX Quantum*

- 3**, 030301 (2022), URL <https://link.aps.org/doi/10.1103/PRXQuantum.3.030301>.
- [28] S. Puri, A. Grimm, P. Campagne-Ibarcq, A. Eickbusch, K. Noh, G. Roberts, L. Jiang, M. Mirrahimi, M. H. Devoret, and S. M. Girvin, *Phys. Rev. X* **9**, 041009 (2019), URL <https://link.aps.org/doi/10.1103/PhysRevX.9.041009>.
- [29] M. Rymarz, S. Bosco, A. Ciani, and D. P. DiVincenzo, *Phys. Rev. X* **11**, 011032 (2021), URL <https://link.aps.org/doi/10.1103/PhysRevX.11.011032>.
- [30] J. Conrad, *Phys. Rev. A* **103**, 022404 (2021), URL <https://link.aps.org/doi/10.1103/PhysRevA.103.022404>.
- [31] G. M. Zaslavskii, M. Y. Zakharov, R. Z. Sagdeev, D. Usikov, and A. A. Chernikov, *Zh. Eksp. Teor. Fiz.* **91**, 500 (1986).
- [32] G. P. Berman, V. Y. Rubaev, and G. M. Zaslavsky, *Nonlinearity* **4**, 543 (1991), URL <https://dx.doi.org/10.1088/0951-7715/4/2/015>.
- [33] P. Leboeuf, J. Kurchan, M. Feingold, and D. P. Arovav, *Phys. Rev. Lett.* **65**, 3076 (1990), URL <https://link.aps.org/doi/10.1103/PhysRevLett.65.3076>.
- [34] P. Leboeuf, J. Kurchan, M. Feingold, and D. P. Arovav, *Chaos: An Interdisciplinary Journal of Nonlinear Science* **2**, 125 (1992), <https://doi.org/10.1063/1.165915>, URL <https://doi.org/10.1063/1.165915>.
- [35] T. P. Billam and S. A. Gardiner, *Phys. Rev. A* **80**, 023414 (2009), URL <https://link.aps.org/doi/10.1103/PhysRevA.80.023414>.
- [36] L. Guo, M. Marthaler, and G. Schön, *Phys. Rev. Lett.* **111**, 205303 (2013), URL <https://link.aps.org/doi/10.1103/PhysRevLett.111.205303>.
- [37] Y. Zhang, J. Gosner, S. M. Girvin, J. Ankerhold, and M. I. Dykman, *Phys. Rev. A* **96**, 052124 (2017), URL <https://link.aps.org/doi/10.1103/PhysRevA.96.052124>.
- [38] P. Liang, M. Marthaler, and L. Guo, *New Journal of Physics* **20**, 023043 (2018), URL <https://doi.org/10.1088/1367-2630/aaa7c3>.
- [39] N. Lörch, Y. Zhang, C. Bruder, and M. I. Dykman, *Phys. Rev. Research* **1**, 023023 (2019), URL <https://link.aps.org/doi/10.1103/PhysRevResearch.1.023023>.
- [40] L. Guo, V. Peano, and F. Marquardt, *Phys. Rev. B* **105**, 094301 (2022), URL <https://link.aps.org/doi/10.1103/PhysRevB.105.094301>.
- [41] S. Rahav, I. Gilyar, and S. Fishman, *Phys. Rev. A* **68**, 013820 (2003), URL <https://link.aps.org/doi/10.1103/PhysRevA.68.013820>.
- [42] N. Goldman and J. Dalibard, *Phys. Rev. X* **4**, 031027 (2014), URL <https://link.aps.org/doi/10.1103/PhysRevX.4.031027>.
- [43] M. Bukov, L. D'Alessio, and A. Polkovnikov, *Advances in Physics* **64**, 139 (2015), <https://doi.org/10.1080/00018732.2015.1055918>, URL <https://doi.org/10.1080/00018732.2015.1055918>.
- [44] F. Casas, J. A. Oteo, and J. Ros, *Journal of Physics A: Mathematical and General* **34**, 3379 (2001), URL <https://doi.org/10.1088/0305-4470/34/16/305>.
- [45] S. Blanes, F. Casas, J. Oteo, and J. Ros, *Physics Reports* **470**, 151 (2009), ISSN 0370-1573, URL <https://www.sciencedirect.com/science/article/pii/S0370157308004092>.
- [46] A. Eckardt and E. Anisimovas, *New Journal of Physics* **17**, 093039 (2015), URL <https://doi.org/10.1088/1367-2630/17/9/093039>.
- [47] T. Mikami, S. Kitamura, K. Yasuda, N. Tsuji, T. Oka, and H. Aoki, *Phys. Rev. B* **93**, 144307 (2016), URL <https://link.aps.org/doi/10.1103/PhysRevB.93.144307>.
- [48] M. Bukov, L. D'Alessio, and A. Polkovnikov, *Advances in Physics* **64**, 139 (2015), <https://doi.org/10.1080/00018732.2015.1055918>, URL <https://doi.org/10.1080/00018732.2015.1055918>.
- [49] M. S. Rudner and N. H. Lindner, *Nature Reviews Physics* **2**, 229 (2020), ISSN 2522-5820, URL <https://doi.org/10.1038/s42254-020-0170-z>.
- [50] M. Scully and M. Zubairy, *Quantum Optics, Quantum Optics* (Cambridge University Press, 1997), ISBN 9780521435956, URL <https://books.google.de/books?id=20ISsQCKKmQC>.
- [51] M. Marthaler and M. I. Dykman, *Phys. Rev. A* **73**, 042108 (2006), URL <https://link.aps.org/doi/10.1103/PhysRevA.73.042108>.
- [52] V. Peano, M. Marthaler, and M. I. Dykman, *Phys. Rev. Lett.* **109**, 090401 (2012), URL <https://link.aps.org/doi/10.1103/PhysRevLett.109.090401>.
- [53] M. Dykman, *Fluctuating Nonlinear Oscillators: From Nanomechanics to Quantum Superconducting Circuits* (Oxford University Press, 2012), ISBN 9780199691388, URL <https://doi.org/10.1093/acprof:oso/9780199691388.001.0001>.
- [54] A. Bachtold, J. Moser, and M. I. Dykman, *Rev. Mod. Phys.* **94**, 045005 (2022), URL <https://link.aps.org/doi/10.1103/RevModPhys.94.045005>.
- [55] R. Bistritzer and A. H. MacDonald, *Proceedings of the National Academy of Sciences* **108**, 12233 (2011), <https://www.pnas.org/doi/pdf/10.1073/pnas.1108174108>, URL <https://www.pnas.org/doi/abs/10.1073/pnas.1108174108>.
- [56] Y. Cao, V. Fatemi, A. Demir, S. Fang, S. L. Tomarken, J. Y. Luo, J. D. Sanchez-Yamagishi, K. Watanabe, T. Taniguchi, E. Kaxiras, et al., *Nature* **556**, 80 (2018), ISSN 1476-4687, URL <https://doi.org/10.1038/nature26154>.
- [57] Y. Cao, V. Fatemi, S. Fang, K. Watanabe, T. Taniguchi, E. Kaxiras, and P. Jarillo-Herrero, *Nature* **556**, 43 (2018), ISSN 1476-4687, URL <https://doi.org/10.1038/nature26160>.
- [58] A. Thomson, S. Chatterjee, S. Sachdev, and M. S. Scheurer, *Phys. Rev. B* **98**, 075109 (2018), URL <https://link.aps.org/doi/10.1103/PhysRevB.98.075109>.
- [59] L. Guo, M. Liu, and M. Marthaler, *Phys. Rev. A* **93**, 053616 (2016), URL <https://link.aps.org/doi/10.1103/PhysRevA.93.053616>.
- [60] L. Guo, in *Phase Space Crystals* (IOP Publishing, 2021), 2053-2563, pp. 4-1 to 4-28, ISBN 978-0-7503-3563-8, URL <https://dx.doi.org/10.1088/978-0-7503-3563-8ch4>.
- [61] K. Sacha, *Scientific Reports* **5**, 10787 (2015), ISSN 2045-2322, URL <https://doi.org/10.1038/srep10787>.
- [62] M. Mierzejewski, K. Giergiel, and K. Sacha, *Phys. Rev. B* **96**, 140201 (2017), URL <https://link.aps.org/doi/10.1103/PhysRevB.96.140201>.
- [63] K. Giergiel, A. Miroszewski, and K. Sacha, *Phys. Rev. Lett.* **120**, 140401 (2018), URL <https://link.aps.org/doi/10.1103/PhysRevLett.120.140401>.
- [64] K. Sacha, *Condensed Matter Physics in the Time Dimension* (Springer International Publishing, Cham, 2020),

- pp. 173–235, ISBN 978-3-030-52523-1, URL https://doi.org/10.1007/978-3-030-52523-1_5.
- [65] L. Guo and P. Liang, *New Journal of Physics* **22**, 075003 (2020), URL <https://doi.org/10.1088/1367-2630/ab9d54>.
- [66] P. Hannaford and K. Sacha, *AAPPS Bulletin* **32**, 12 (2022), ISSN 2309-4710, URL <https://doi.org/10.1007/s43673-022-00041-8>.
- [67] H. Moritz, T. Stöferle, M. Köhl, and T. Esslinger, *Phys. Rev. Lett.* **91**, 250402 (2003), URL <https://link.aps.org/doi/10.1103/PhysRevLett.91.250402>.
- [68] Z. Hadzibabic, S. Stock, B. Battelier, V. Bretin, and J. Dalibard, *Phys. Rev. Lett.* **93**, 180403 (2004), URL <https://link.aps.org/doi/10.1103/PhysRevLett.93.180403>.
- [69] F. Chen, J. Li, A. D. Armour, E. Brahim, J. Stettenheim, A. J. Sirois, R. W. Simmonds, M. P. Blencowe, and A. J. Rimberg, *Phys. Rev. B* **90**, 020506 (2014), URL <https://link.aps.org/doi/10.1103/PhysRevB.90.020506>.
- [70] M. Hofheinz, F. Portier, Q. Baudouin, P. Joyez, D. Vion, P. Bertet, P. Roche, and D. Esteve, *Phys. Rev. Lett.* **106**, 217005 (2011), URL <https://link.aps.org/doi/10.1103/PhysRevLett.106.217005>.
- [71] F. Chen, A. J. Sirois, R. W. Simmonds, and A. J. Rimberg, *Applied Physics Letters* **98**, 132509 (2011).
- [72] A. D. Armour, M. P. Blencowe, E. Brahim, and A. J. Rimberg, *Phys. Rev. Lett.* **111**, 247001 (2013), URL <https://link.aps.org/doi/10.1103/PhysRevLett.111.247001>.
- [73] V. Gramich, B. Kubala, S. Rohrer, and J. Ankerhold, *Phys. Rev. Lett.* **111**, 247002 (2013), URL <https://link.aps.org/doi/10.1103/PhysRevLett.111.247002>.
- [74] J. Leppäkangas, G. Johansson, M. Marthaler, and M. Fogelström, *Phys. Rev. Lett.* **110**, 267004 (2013), URL <https://link.aps.org/doi/10.1103/PhysRevLett.110.267004>.
- [75] J. Leppäkangas, M. Fogelström, A. Grimm, M. Hofheinz, M. Marthaler, and G. Johansson, *Phys. Rev. Lett.* **115**, 027004 (2015), URL <https://link.aps.org/doi/10.1103/PhysRevLett.115.027004>.
- [76] J. Leppäkangas, M. Fogelström, M. Marthaler, and G. Johansson, *Phys. Rev. B* **93**, 014506 (2016), URL <https://link.aps.org/doi/10.1103/PhysRevB.93.014506>.
- [77] A. D. Armour, B. Kubala, and J. Ankerhold, *Phys. Rev. B* **91**, 184508 (2015), URL <https://link.aps.org/doi/10.1103/PhysRevB.91.184508>.
- [78] M. Trif and P. Simon, *Phys. Rev. B* **92**, 014503 (2015), URL <https://link.aps.org/doi/10.1103/PhysRevB.92.014503>.
- [79] B. Kubala, V. Gramich, and J. Ankerhold, *Physica Scripta* **T165**, 014029 (2015), URL <https://doi.org/10.1088/0031-8949/2015/t165/014029>.
- [80] P. P. Hofer, J.-R. Souquet, and A. A. Clerk, *Phys. Rev. B* **93**, 041418 (2016), URL <https://link.aps.org/doi/10.1103/PhysRevB.93.041418>.
- [81] S. Dambach, B. Kubala, and J. Ankerhold, *New Journal of Physics* **19**, 023027 (2017), URL <https://doi.org/10.1088/1367-2630/aa5bb6>.
- [82] B. Lang and A. D. Armour, *New Journal of Physics* **23**, 033021 (2021), URL <https://doi.org/10.1088/1367-2630/abe483>.
- [83] B. Lang, G. F. Morley, and A. D. Armour, *Discrete time translation symmetry breaking in a josephson junction laser* (2022), URL <https://arxiv.org/abs/2208.03191>.
- [84] L. Guo and M. Marthaler, *New Journal of Physics* **18**, 023006 (2016), URL <https://doi.org/10.1088/1367-2630/18/2/023006>.
- [85] H. Srivastava and J. Choi, in *Zeta and q-Zeta Functions and Associated Series and Integrals*, edited by H. Srivastava and J. Choi (Elsevier, London, 2012), pp. 1–140, ISBN 978-0-12-385218-2, URL <https://www.sciencedirect.com/science/article/pii/B9780123852182000013>.
- [86] R. N. Bracewell, *Australian Journal of Physics* **9**, 198 (1956), URL <https://doi.org/10.1071/PH560198>.
- [87] R. Ng, *ACM Trans. Graph.* **24**, 735–744 (2005), ISSN 0730-0301, URL <https://doi.org/10.1145/1073204.1073256>.
- [88] G. B. Arfken and H. J. Weber, *Mathematical Methods for Physicists* (Academic Press; 6th edition, 2005), ISBN 978-0120598762.